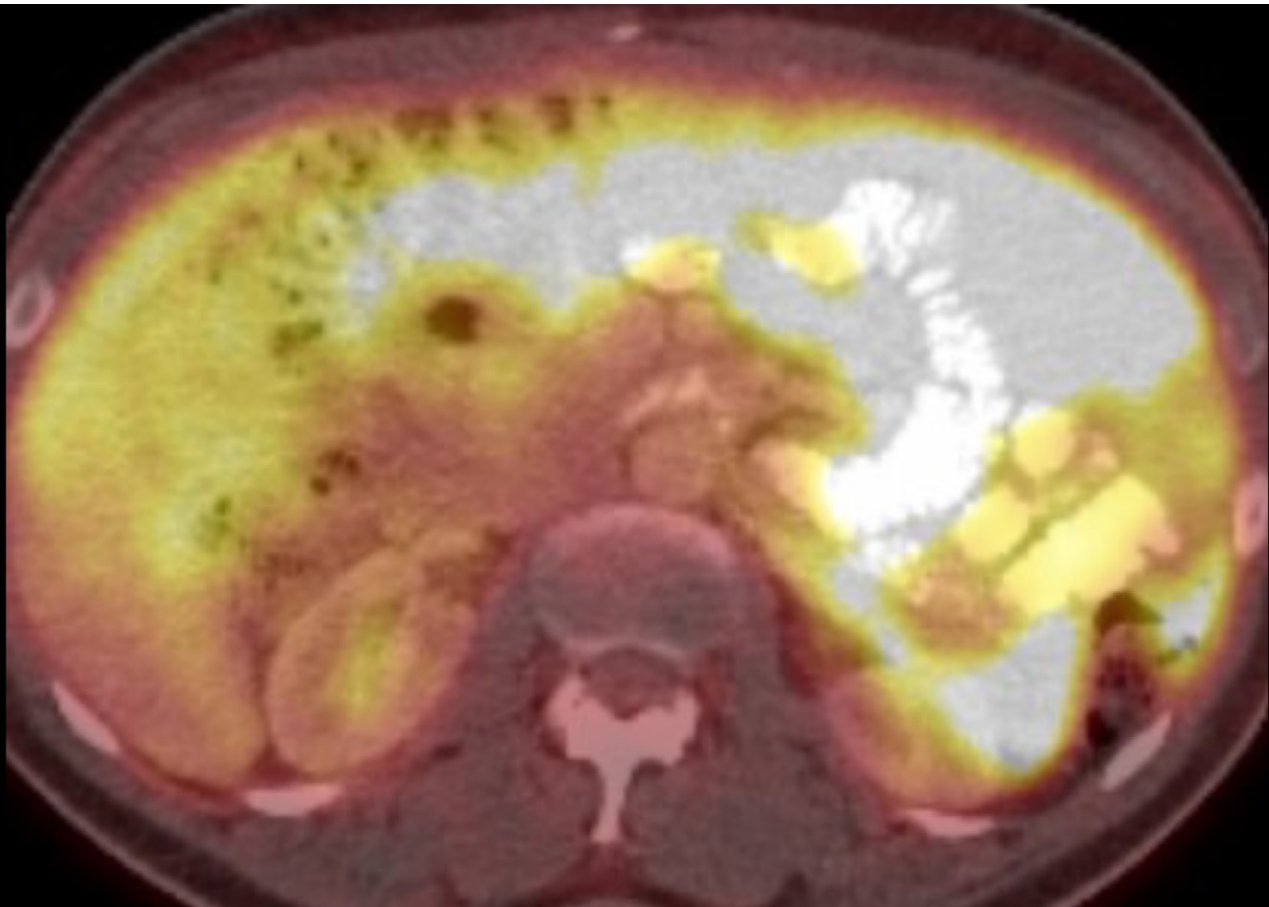


# The Peritoneum: Anatomy, Pathologic Findings, and Patterns of Disease Spread

Ayman H. Gaballah, MD • Maged Algazzar, MD • Irfan A. Kazi, MD • Mohamed Badawy, MD • Nicholas Philip Guys, MD  
Eslam Adel Shehata Mohamed, MD • Jennifer Sammon, MD • Khaled M. Elsayes, MD • Peter S. Liu, MD • Matthew Heller, MD

Author affiliations, funding, and conflicts of interest are listed at [the end of this article](#).



Disease spread in the abdomen and pelvis generally occurs in a predictable pattern in relation to anatomic landmarks and fascial planes. Anatomically, the abdominopelvic cavity is subdivided into several smaller spaces or compartments by key ligaments and fascial planes. The abdominal cavity has been traditionally divided into peritoneal, retroperitoneal, and pelvic extraperitoneal spaces. Recently, more clinically relevant classifications have evolved. Many pathologic conditions affect the abdominal cavity, including traumatic, inflammatory, infectious, and neoplastic processes. These abnormalities can extend beyond their sites of origin through various pathways. Identifying the origin of a disease process is the first step in formulating a differential diagnosis and ultimately reaching a final diagnosis. Pathologic conditions differ in terms of pathways of disease spread. For example, simple fluid tracks along fascial planes, respecting anatomic boundaries, while fluid from acute necrotizing pancreatitis can destroy fascial planes, resulting in transfascial spread without regard for anatomic landmarks. Furthermore, neoplastic processes can spread through multiple pathways, with a propensity for spread to noncontiguous sites. When the origin of a disease process is not readily apparent, recognizing the spread pattern can allow the radiologist to work backward and ultimately arrive at the site or source of pathogenesis. As such, a cohesive understanding of the peritoneal anatomy, the typical organ or site of origin for a disease process, and the corresponding pattern of disease spread is critical not only for initial diagnosis but also for establishing a road map for staging, anticipating further disease spread, guiding search patterns and report checklists, determining prognosis, and tailoring appropriate follow-up imaging studies.

©RSNA, 2024 • [radiographics.rsna.org](http://radiographics.rsna.org)

Supplemental  
MaterialTest Your  
Knowledge

RadioGraphics 2024; 44(8):e230216  
<https://doi.org/10.1148/rg.230216>

Content Codes: CT, GI

## TEACHING POINTS

- A solid understanding of peritoneal anatomy coupled with a knowledge of the nature and origin of the most common peritoneal abnormalities can facilitate a deeper understanding of how these disease processes spread and the factors involved in limiting such spread.
- Spread of disease in the peritoneal cavity occurs along specific anatomic pathways created by the peritoneal ligaments, folds, and recesses and is influenced by peritoneal fluid flow dynamics. Sites of preferential fluid stasis and variable fluid reabsorption also influence spread.
- Identifying the peritoneal and mesenteric ligaments characteristically involved in a disease process and knowing their anatomic connections are crucial to systematically assessing disease spread.
- The portal vein runs in the hepatoduodenal ligament and can be affected by neoplastic and nonneoplastic disease processes. In cases of advanced cancers, dissection of the hepatoduodenal ligament with preservation of the portal vein and hepatic artery has a high risk of leaving residual tumor and portends a poor prognosis.
- Tumor cells from primary bowel malignancies may limit or obstruct flow in adjacent lymphatic vessels. On CT images, this can manifest as bowel wall thickening and edema, thickened mucosal folds, loss of colonic haustrations, and increased attenuation, or stranding, of surrounding mesenteric fat.

## Introduction

The abdominopelvic cavity is the largest body compartment and is subdivided into several smaller spaces by key ligaments and fascial planes. Traditionally, the cavity is divided into peritoneal, retroperitoneal, and extraperitoneal spaces (1). Disease spread within the peritoneum and peritoneal spaces generally follows a predictable pattern influenced by two key factors: the anatomic organization of the compartments and the specific nature of the disease process.

A myriad of disease processes can affect the peritoneum and its subspaces, including extraluminal gas, fluid collections, localized or generalized inflammation, diverse infections, and a wide range of neoplastic processes, among many others. Pathologic conditions may extend beyond their sites of origin through numerous channels, including direct extension, hematogenous or lymphatic spread, spread along the mesenteries and ligaments, and spread along perivascular and perineural pathways (2).

A solid understanding of peritoneal anatomy coupled with a knowledge of the nature and origin of the most common peritoneal abnormalities can facilitate a deeper understanding of how these disease processes spread and the factors involved in limiting such spread. Conversely, when the origin of a disease is not known, the manner of spread can serve as a helpful clue in determining the nature and source of the abnormality. A systematic approach enables radiologists to develop effective search patterns and reporting checklists and to minimize errors. This review delineates the most common patterns of peritoneal disease spread and how they relate to important anatomic structures.

## Anatomy of the Peritoneum

Knowledge of basic peritoneal embryologic development (Fig S1) is important for understanding mechanisms and pathways of disease spread in the abdomen and pelvis. The peritoneum, which is lined by a single layer of mesothelial cells, is the largest serous membrane in the body. It comprises separate parietal and visceral layers, with an intervening potential space known as the peritoneal cavity. The parietal peritoneum lines the walls of the abdominal cavity, while the visceral peritoneum envelops the gastrointestinal viscera. Familiarity with the anatomy and anatomic landmarks, such as peritoneal ligaments, cavities, and spaces, is important (3,4).

### Peritoneal Ligaments and Derivatives

Peritoneal ligaments represent two layers of visceral peritoneum doubled back on themselves. They are key for supporting organs and other structures in the peritoneal cavity and providing a point of attachment to the abdominal wall and each other. Furthermore, these ligaments anchor and stabilize the organs in position and provide a pathway or conduit for blood vessels, nerves, and lymphatic vessels to enter and exit the organs. As such, they can also act as both a conduit and a barrier for disease spread (3–5).

Many peritoneal ligaments are named according to the organs they connect (Figs 1, 2, S2–S4). Mesenteries and omenta are specific peritoneal ligaments related to the bowel and the stomach, respectively (6). At imaging, peritoneal ligaments are typically identified by the blood vessels running through them at characteristic anatomic locations (Figs 1, 2, S2–S4) (7). Table 1 summarizes these ligaments, their attachments, and their important imaging landmarks (6,8,9).

### Peritoneal Cavity and Spaces

In male patients, the peritoneal cavity is closed, whereas in female patients, it communicates with the extraperitoneal space through the fallopian tubes and reproductive organs (10). Normally, the peritoneal cavity is collapsed, and the two layers are imperceptible on cross-sectional images. However, in various disease states, the individual peritoneal layers can be visualized, especially when the cavity is distended with fluid (11). The peritoneal cavity is subdivided into supra- and inframesocolic compartments by the transverse mesocolon (Figs 3, S5) (1,6).

The supramesocolic compartment includes the spaces formed secondary to the peritoneal attachments between the abdominal portions of the esophagus, stomach, liver, spleen, the adjacent anterior and posterior abdominal wall, and the overlying diaphragm. The falciform ligament further subdivides the supramesocolic space into left and right supramesocolic spaces. The right supramesocolic space involves the right subphrenic and subhepatic spaces and the lesser sac. The lesser omentum forms the border between the subhepatic space and the lesser sac, where the two communicate through the foramen of Winslow or epiploic foramen. The right subhepatic space is further subdivided into anterior and posterior (Morison pouch) spaces (Figs 3, S5) (6).

The left supramesocolic space is divided into the left subphrenic and left perihepatic (subhepatic) spaces. The left

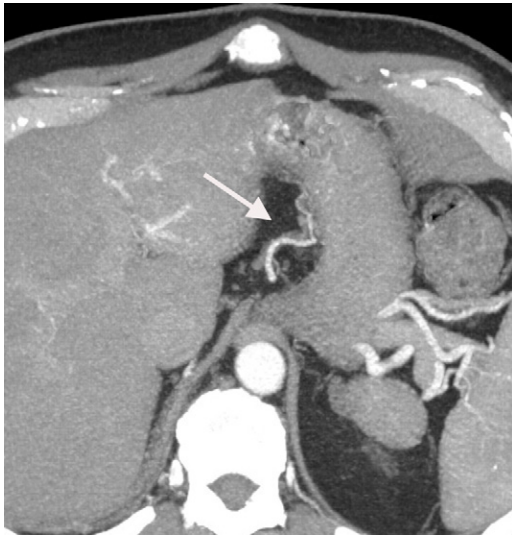


**Figure 1.** Normal anatomy of the gastrohepatic ligament in a 55-year-old man. Axial contrast-enhanced CT image of the abdomen shows the fat plane between the lesser curvature of the stomach and the liver (arrow), representing the gastrohepatic ligament. The left gastric artery serves as a landmark for identification of the ligament..

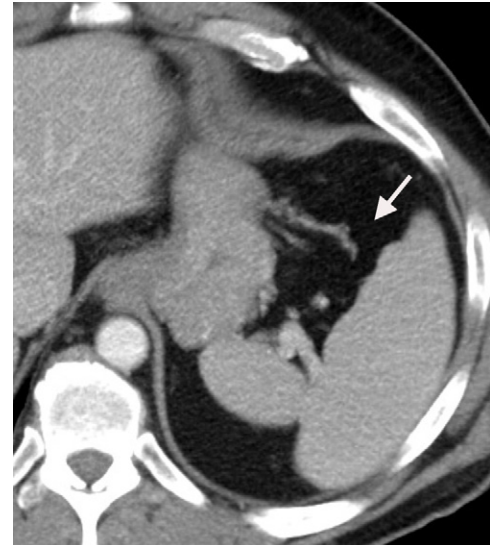


**Figure 2.** Normal anatomy of the gastro-splenic ligament in a 56-year-old man. Axial contrast-enhanced CT image of the abdomen shows the fat plane between the spleen and the greater curvature of the stomach (arrow). The short gastric and left gastroepiploic vessels course through the ligament and together represent the anatomic landmarks for the ligament.

subhepatic space is divided into the left anterior and posterior subhepatic spaces. The left posterior subhepatic space or gastrohepatic recess is between the left hepatic lobe and the stomach (4,8).

The inframesocolic compartment is divided by the obliquely oriented small bowel mesentery into the right and left infracolic spaces and right and left paracolic gutters (Figs 3, S5). Right infracolic fluid collections are limited inferiorly by the small bowel mesentery attachment at the ileocecal junction, while the left infracolic space communicates freely with the pelvis. The right and left paracolic gutters lie lateral to the ascending and descending colon, respectively. The right paracolic gutter maintains continuity with the right supramesocolic space superiorly (Figs 4, S6), while the left paracolic gutter is partially separated from the left supramesocolic space by the phrenicocolic ligament (Figs 4, S6) (5,11–13).

### Perspectives and Models of Abdominal Cavity Anatomy

Many perspectives exist regarding abdominopelvic cavity anatomy, and several models have been used to describe anatomic foundations. These models include the traditional peritoneal-based model, the peritoneal and subperitoneal space model (ie, the “holistic approach”), and the more recent mesenteric-based model, which are discussed individually in Table 2 (1,6,14–18).

#### Traditional Model

The traditional or peritoneal-based model has been used to categorize organs as either intraperitoneal or extraperitoneal (Table 2). This approach views the abdominal cavity as confined spaces delineated by a complex interconnected network of peritoneal derivatives such as peritoneal ligaments,

folds, mesenteries, and omenta as well as other fascial planes (14,15). The traditional approach is helpful in localizing disease processes and providing a differential diagnosis of related abnormalities. However, it is limited in explaining pathways of disease spread (17,19).

#### Holistic Model

The holistic model or subperitoneal approach, proposed by Meyers (2), subdivides the abdominal cavity into a peritoneal cavity and a subperitoneal space (Table 2) (Fig S7). The peritoneal cavity contains no organs. The subperitoneal space contains the abdominopelvic viscera and mesenteric derivatives (eg, the omenta and ligaments) as well as the extraperitoneal spaces (Fig S7). Transperitoneal disease spread occurs when a disease crosses the peritoneal membrane, accounting for bidirectional disease spread between the peritoneal cavity and subperitoneal spaces. The holistic model is more useful for illustrating disease spread (2).

#### Mesenteric and Nonmesenteric Domains Model

The recent reclassification of the mesentery as a distinct organ has led to the development of a new model for conceptualizing abdominal and pelvic anatomy (9,16). Studies (16,17) have shown that the embryonic mesentery, believed to be fragmented per the traditional model, demonstrates continuity from the gastroesophageal junction to the rectum into adulthood. This model classifies the abdominopelvic cavity into mesenteric and nonmesenteric domains. The mesenteric domain encompasses the mesentery and all digestive organs from the gastroesophageal junction to the level of the mesorectum. The nonmesenteric domain involves the genitourinary organs,

**Table 1: Peritoneal Ligaments: Extensions and Contents**

Ligament	Identifying Imaging Features	
	Extension and Features	Structural Contents
Transverse mesocolon	Extends from the transverse colon to the pancreas	Middle colic vessels Gastrocolic trunk
Supramesocolic peritoneal ligaments		
Gastrohepatic ligament	Fatty plane between the lesser curvature of the stomach and the left hepatic lobe	Left gastric artery Left gastric or coronary vein
Hepatoduodenal ligament	Hepatic hilum to the flexure between the first and second parts of the duodenum	Portal vein Hepatic artery Common bile duct
Gastrosplenic ligament	Superior one-third of the greater curvature of the stomach to the splenic hilum	Short gastric vessels Left gastroepiploic vessels
Splenorenal ligament	Splenic hilum to the left anterior pararenal space	Splenic vessels near hilum and pancreatic tail
Gastrocolic ligament (greater omentum)	Inferior two-thirds of the greater curvature of the stomach to the transverse colon	Right and left gastroepiploic vessels
Falciform ligament	Attaches the liver to the diaphragm and anterior abdominal wall	Ligamentum teres (remnant of umbilical vein)
Inframesocolic peritoneal ligaments		
Small bowel mesentery	Extends obliquely from the duodenojejunal junction to the right iliac fossa	Superior mesenteric vessels
Duodenocolic ligament	Extends from the duodenum to the hepatic flexure	...
Phrenicocolic ligament	Extends from the splenic flexure to the diaphragm	...
Ascending mesocolon	Extends from the ascending colon to the root of the small bowel mesentery	Right colic and ileocolic vessels
Descending mesocolon	Extends from the descending colon to the root of the small bowel mesentery	Left colic vessels
Sigmoid mesocolon	Sigmoid colon to pelvic wall	Sigmoid vessels Marginal vessels Superior rectal vessels
Broad ligament	Attaches lateral uterus to lateral pelvic sidewalls	Uterine and ovarian vessels Ovaries and fallopian tubes

Note.—The gastrohepatic and hepatoduodenal ligaments form the lesser omentum.

musculoskeletal frame, and great vessels. Researchers believe this relatively new model will enhance our comprehension of abdominal compartmentalization. It may also offer valuable insights for clinical decision making and surgical planning (9).

### Pathophysiologic Characteristics and Flow Dynamics of Peritoneal Fluid

Peritoneal fluid is constantly produced and absorbed by the peritoneum and is maintained in a dynamic equilibrium regulated by the lymphatic system. Under normal physiologic conditions, 25–50 mL of fluid is present in the peritoneal cavity of adults (20,21).

The distribution and typical flow patterns of peritoneal fluid depend on a number of factors, including the site, origin, rate of accumulation, and density of the fluid; the presence of peritoneal adhesions; the degree of urinary bladder distention; intraperitoneal pressure; and patient positioning, as well as the normal anatomic divisions of the peritoneal cavity created by the peritoneal ligaments and mesenteries (18,21,22).

Spread of disease in the peritoneal cavity occurs along specific anatomic pathways created by the peritoneal ligaments, folds, and recesses and is influenced by peritoneal fluid flow dynamics (Fig 5). Sites of preferential fluid stasis and variable fluid reabsorption also influence spread. Peritoneal fluid circulates by means of a combination of downward movement by gravity and upward movement driven by subdiaphragmatic negative pressure (18). During inspiration, subdiaphragmatic pressure decreases, causing peritoneal fluid to move cranially toward the diaphragm and along the paracolic gutters. Free flow through the left paracolic gutter is hindered by the phrenicocolic ligament, while the right paracolic gutter serves as a major bidirectional pathway for the spread of disease between the upper and lower abdominal cavity. Consequently, subphrenic and subhepatic abscesses and peritoneal deposits are observed more frequently on the right side than on the left side (Figs 6, S6) (23). Areas of fluid stasis favor fluid accumulation and seeding of peritoneal deposits. These include the rectovesical and rectouterine pouches, the right lower quadrant in the ileocolic region along the attachment of

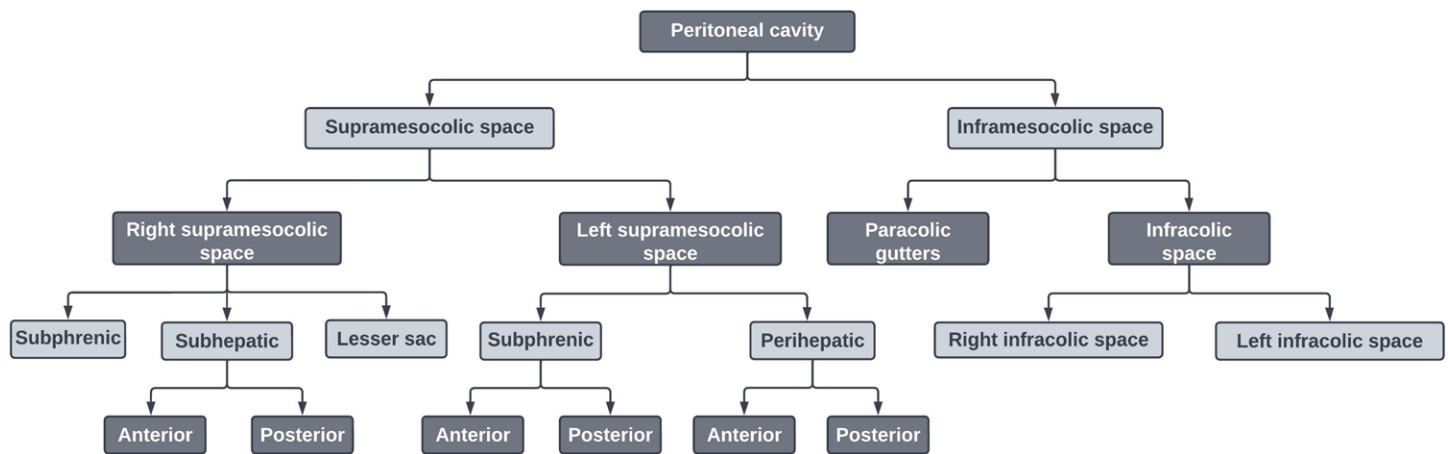


**Figure 3.** Flowchart shows the different spaces in the peritoneal cavity.



**Figure 4.** Anatomy of the peritoneal cavity in a 47-year-old woman. Coronal contrast-enhanced CT image shows contrast material leakage into the peritoneal cavity, demonstrating the continuity of the right supramesocolic space with the right paracolic gutter (black arrowheads). The phrenocolic ligament (arrow) partially separates the left supramesocolic space and the left paracolic gutter (white arrowheads) posteriorly.

the small bowel mesentery, the left lower quadrant along the superior border of the sigmoid mesocolon, the right paracolic gutter, and the right subphrenic space (Figs 6, S6). Careful examination of these sites allows accurate evaluation of the spread of disease and anticipation of the development of peritoneal deposits or abscesses (24). An especially pertinent example of the influence of fluid flow and redistribution is mucinous ascites, which tends to affect the hepatic surface and the right subphrenic space (Fig 7) (25).

The rectouterine pouch, also known as the pouch of Douglas in females and the rectovesical pouch in males, represents the most gravity-dependent intraperitoneal space for an upright patient. Conversely, the dorsal right subhepatic space (also known as the Morison pouch or the hepatorenal recess)

is the most dependent space in the upper abdominal cavity for a supine patient. These sites commonly serve as locations for free (nonloculated) intraperitoneal fluid collections and for developing peritoneal metastases, particularly in bedridden patients (26).

### Pathologic Findings and Patterns of Disease Spread

A wide variety of disease processes can involve both the peritoneal membrane and its many spaces (26–30). These abnormalities can propagate at and/or away from their site of origin through various routes, including dissemination throughout the peritoneal cavity, direct extension, extension along the mesenteries and ligaments, lymphatic or perilymphatic spread, perivascular and perineural spread, and hematogenous spread (2). Factors such as disease aggressiveness, site of origin, and structures facilitating or impeding communication between the many abdominal and pelvic compartments influence how such a disease propagates. Major abnormalities involving the peritoneal cavity, peritoneal membrane, and peritoneal derivatives, including their main pathways of spread, are discussed in the following sections. Primary diseases of the visceral organs are beyond the scope of this review.

### Peritoneal Membrane and Cavity

Major peritoneal cavity or membrane abnormalities include free air, free and organized fluid collections, and primary and secondary malignancies.

**Extraluminal Gas.**—Free air in the peritoneal cavity is often an important sign of bowel perforation (27). Additional causes of pneumoperitoneum include trauma, recent surgery or other interventions, and infection by gas-producing organisms (Fig 8). It is important to rule out postoperative and postprocedural causes and findings that may cause extraluminal peritoneal air. Pneumoperitoneum is an expected normal finding in the early postoperative period, demonstrating a progressive decrease in volume at follow-up imaging. It usually resolves within 3–4 days but occasionally persists for 3–4 weeks. Increasing pneumoperitoneum or a lack of gradual resolution in the postoperative period are indicators of complications

**Table 2: Different Models and Perspectives of Abdominopelvic Cavity Anatomy**

Model and Compartments	Salient Features
Traditional model	Divides abdominopelvic cavity into intraperitoneal and extraperitoneal compartments
Intraperitoneal compartment	Peritoneal cavity, subdivided into communicating spaces by peritoneal ligaments Peritoneal ligaments, folds, mesenteries, and omenta Gastrointestinal organs that are totally covered by the visceral peritoneum: the liver, spleen, and mobile portions of the bowel (stomach, jejunum, ileum, transverse colon, and sigmoid colon)
Extraperitoneal compartment	The preperitoneal space, which is anterolateral to the anterior parietal peritoneum The retroperitoneum, which is bounded anteriorly by the posterior parietal peritoneum and by the transversalis fascia posteriorly The non-mobile portions of the bowel (duodenum, ascending and descending colon), their corresponding retroperitonealized portions of the mesentery, and the pancreas are located within the retroperitoneum, namely in the anterior pararenal space The pelvic extraperitoneal space
Holistic model (reference 2)	Compartmentalizes abdominal cavity into two mutually exclusive spaces: peritoneal cavity and subperitoneal space separated by the peritoneum; each space is considered as an interconnected anatomic continuum This perspective helps in predicting disease spread, progression, and prognosis
Peritoneal cavity	Potential space enclosed by the peritoneal layers and devoid of organs
Subperitoneal space: a single interconnected space	All the abdominal and pelvic organs, their blood vessels, lymphatics, and nerve supply Mesenchymal connective tissue, including mesenteries, omenta, and ligaments Extraperitoneal spaces
Mesenteric model	Compartmentalizes the abdomen and pelvis into mesenteric and nonmesenteric domains
Mesenteric domain	Contains all the gastrointestinal organs arranged on a mesenteric frame As in the traditional model, the mobile portions of the mesentery are enveloped by the peritoneum, while the nonmobile portions have peritoneal lining along their anterior aspect only; in contrast to the traditional model, the contents of the anterior pararenal space (nonmobile portions of the bowel and related mesenteries as well as the pancreas) are considered part of the mesenteric domain
Nonmesenteric domain	Contains the genitourinary organs arranged on a musculoskeletal frame and the great vessels

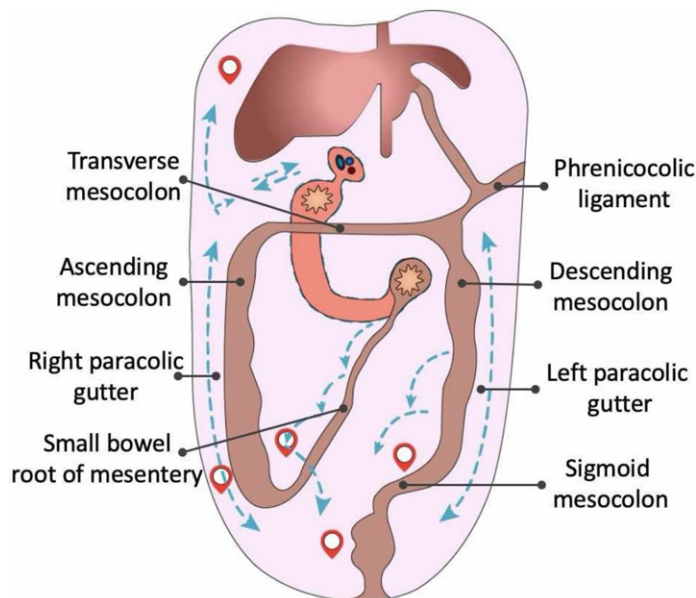


**Figure 5.** Illustration shows the peritoneal spaces and peritoneal fluid flow pattern and the sites of preferential stasis and intraperitoneal seeding.

such as anastomotic leakage, perforation, or sepsis, especially when they are associated with signs of peritonitis. Early identification and intervention are vital to prevent further adverse events (31–33).

Occasionally, the location of peritoneal air indicates the site of perforation. Isolated supramesocolic air is often caused by duodenal or gastric ulcer perforation (Fig 9). The presence of extraluminal gas in the hepatoduodenal ligament is highly suggestive of gastroduodenal perforation. Free air located predominantly in the inframesocolic space and in the mesentery is often related to small bowel or sigmoid colonic perforation (27,34). Secondary signs may help in localizing the site of perforation in difficult cases. These include localized fluid collections, mesenteric stranding, focal bowel wall thickening, a focal bowel wall defect, and pneumatosis (31,32,34,35).

CT is sensitive for detection of free peritoneal air (Fig 9) because even tiny locules of extraluminal gas can be detected. In addition, CT can be useful in determining or at least suggesting a potential site of bowel perforation, guided by the pattern of gas distribution in the peritoneal cavity (Figs 8, 9) (31,32,35). Reviewing CT images with lung windows is especially useful for detecting free intraperitoneal air (33). The peritoneal recess between the liver and diaphragm is often a good place to begin the search for pneumoperitoneum (Fig 9). Extraluminal air can also occur outside the peritoneal cavity and is known as pneumoretroperitoneum (36).

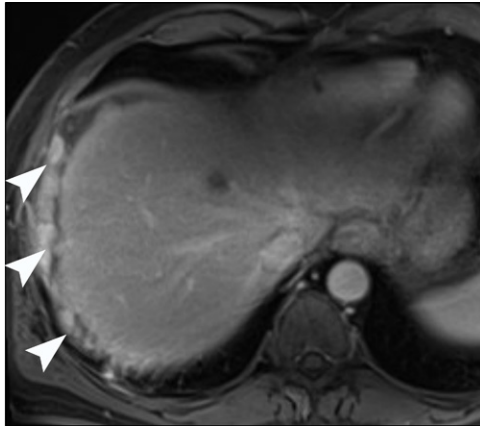


**Figure 6.** Right perihepatic and subphrenic peritoneal deposits in a 67-year-old man with pancreatic adenocarcinoma. Axial contrast-enhanced T1-weighted volumetric interpolated breath-hold examination (VIBE) MR image shows multiple nodular peritoneal metastases in the right subphrenic and perihepatic spaces (arrowheads) with mild associated perihepatic ascites.



**Figure 7.** Intraoperative pseudomyxoma peritonei due to appendiceal mucinous adenocarcinoma in a 66-year-old woman. Axial contrast-enhanced CT image of the upper abdomen shows multiple low-attenuation lesions involving the lesser omentum (curved black arrow); the gastrosplenic ligament (straight black arrow); and subhepatic, perihepatic, and perisplenic spaces (white arrows). The lesions cause mass effect on adjacent structures and characteristic “scalloping” of the liver surface (arrowheads), in addition to central displacement of small bowel loops and the mesentery (not shown).

**Fluid Collections.**—Several diseases are associated with ascites, or the accumulation of free fluid in the peritoneal cavity. Ascites is classified into transudative and exudative subtypes based on the protein content and biochemical composition of the fluid (Table 3) (22,37,38). Common causes of accumulation of transudative ascitic fluid include cirrhosis, congestive heart failure, nephrotic syndrome, and low-protein states, among many others. Infections, inflammatory processes, and malignancy, especially in patients with peritoneal carcinomatosis, are common causes of exudative ascites (Figs 7, 10, S6). Other causes include hemorrhagic (Fig 11), urinary, enteric, bilious, and chylous fluid collections (37,39–42). Certain imaging features can be used to distinguish the various types of peritoneal fluid collections (Table 4) (22,37–43). Transudative fluids generally spread throughout the peritoneal cavity, while exudative fluids are usually more localized and remain near the epicenter of the disease process (Fig 11) (22).

When peritoneal collections are encountered at imaging, a thorough assessment of their location, distribution, imaging features, and associated findings such as the appearance of the peritoneal lining is important for formulating a diagnosis (Table 4). A diagnosis or differential diagnosis can be established by correlating imaging findings with relevant clinical data, thereby guiding management and providing insights into potential extension of the underlying abnormality (37,39,40).

In cases of intra-abdominal hemorrhage, the site of greatest accumulation and pattern of spreading are important to identifying the source of bleeding. The “sentinel clot” sign, for example, is a valuable radiologic sign for determining a source of bleeding. It refers to the presence of hyperattenuating, acutely clotted blood in close proximity to the source, with lower-attenuation nonclotted blood found more distantly (28). This sign is especially useful in cases of slow or prolonged bleeding or when nonenhanced CT is performed.

Inflammatory fluid collections are typically distributed locally near their sites of origin. The presence of loculated ascites

usually indicates the presence of inflammation, infection, or neoplastic processes (22). A fluid collection in the right upper quadrant after a recent biliary intervention or surgery should raise suspicion for a biloma, which can be confirmed using MRI with hepatobiliary contrast agents or with a nuclear medicine hepatobiliary iminodiacetic acid (HIDA) examination. In some cases, direct fluid sampling and laboratory analysis may be necessary for confirmation (42,44).

**Peritoneal Neoplasms.**—Peritoneal neoplasms refer to tumors that involve the peritoneal membranes or cavity. They can be primary, originating in the peritoneum itself, or secondary, spreading from other organs in the abdomen or from distant sites (26,30,45–47). Neoplastic peritoneal lesions manifest with varying degrees of peritoneal thickening and soft-tissue infiltration, mass-forming lesions, ascites, and calcifications (Table 5) (26,29,48). Primary peritoneal malignancies are rare neoplasms originating from the mesothelium or submesothelial tissues (Figs 12, 13) (30,48). The nomenclature of primary peritoneal neoplasms often creates confusion due to the many different names assigned to these tumors, reflecting our evolving understanding of their pathogenesis (46). In general, peritoneal malignancies often come with a delayed diagnosis due to their insidious clinical presentations.

Peritoneal metastatic disease is the most common cause of peritoneal neoplasms. Metastases may originate from epithelial cells (termed *peritoneal carcinomatosis*) (Figs 7, 14), mesenchymal cells (peritoneal sarcomatosis) (Fig S8), or lymphoid cells (peritoneal lymphomatosis) (Figs 15, S9) (Table 5) (30,45).

*Peritoneal carcinomatosis* is defined as seeding or dissemination of malignant epithelial cells into the peritoneal cavity. The most commonly implicated primary tumors are those of gastric, colonic, appendiceal, pancreatic, biliary tract, and ovarian origin (Figs 7, 14, S6, S10). As such, these organs should be carefully examined when peritoneal carcinomatosis is encountered

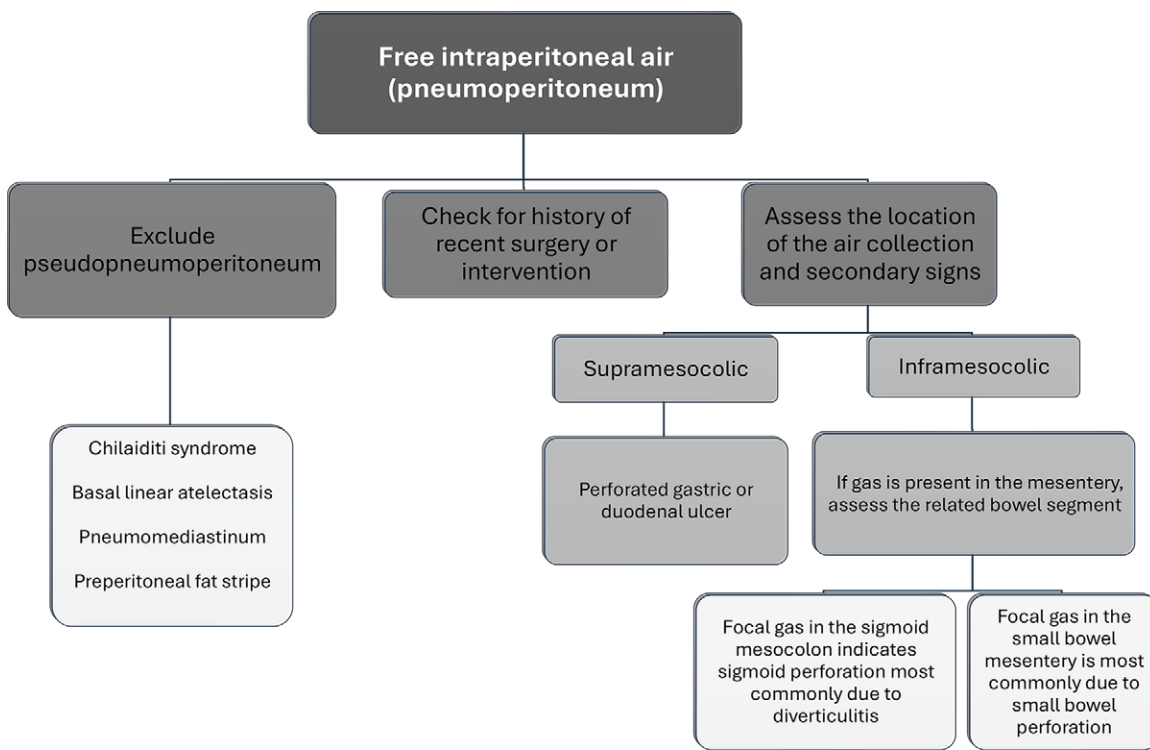


**Figure 8.** Flowchart shows the causes of and diagnostic approaches to pneumoperitoneum.



**Figure 9.** Free intraperitoneal air and peritonitis in a 94-year-old woman with a perforated prepyloric gastric ulcer. Axial contrast-enhanced CT image shows prehepatic free intraperitoneal air (arrow), peritoneal free fluid, and enhancement of the parietal (arrowhead) and perihepatic visceral peritoneal layers, indicating associated peritonitis.

without a known source or origin (48). Imaging features of peritoneal carcinomatosis vary. Common findings include thickening and/or enhancement of the peritoneal layers, peritoneal implants in the form of either peritoneal surface nodularity or discrete masses, and sheetlike growth or infiltration along the mesentery or omenta (Figs 7, 14, 16, S6). Smaller implants may only be recognized as mild fat stranding or peritoneal thickening at imaging. Ascites is an early and common feature of peritoneal carcinomatosis, especially when other causes of free fluid are not evident (Figs 14, S6) (26,48).

A few specific imaging features can help to identify the source of peritoneal implants. For instance, calcified peritoneal deposits in the absence of chemotherapy are usually secondary to a serous ovarian neoplasm (Fig 17) or mucinous tumors of

the stomach, colon, or appendix (24,49). Accurate assessment of the primary tumor and the extent of peritoneal disease is important both for estimating prognosis and for choosing appropriate candidates for therapies such as cytoreductive surgery and hyperthermic intraperitoneal chemotherapy (26,45,46).

Certain nonneoplastic peritoneal lesions, such as inflammatory conditions, infections, benign masses, and masslike lesions, can mimic the appearance and clinical presentation of peritoneal carcinomatosis. Tuberculous peritonitis is an important mimic of peritoneal carcinomatosis (Fig 18). This entity should be suspected when the ileocecal junction is involved in a patient with mesenteric and retroperitoneal lymphadenopathy (especially enlarged lymph nodes with peripheral enhancement and central low attenuation). In contrast to carcinomatosis, tuberculous peritonitis often causes smooth uniform peritoneal thickening (Fig 18). These findings, especially when combined with other ancillary findings, such as calcified granulomas in the liver and spleen and pulmonary or mediastinal manifestations, can be helpful clues to a diagnosis of tuberculous peritonitis (26,45,50).

Peritoneal splenosis can appear as well-defined peritoneal masses mimicking peritoneal metastases. A clinical history of splenic trauma or surgery and imaging characteristics of the masses should raise the concern for splenosis. The diagnosis can be confirmed with MRI using a contrast agent with ultrasmall superparamagnetic iron oxide particles (ie, ferumoxytol) or specific nuclear medicine examinations such as a technetium 99m (<sup>99m</sup>Tc)-labeled red blood cell study or <sup>99m</sup>Tc sulfur colloid scan (51,52).

Encapsulating peritoneal sclerosis, also known as “abdominal cocoon,” is a rare condition characterized by partial or complete encasement of the small bowel loops by a thick fibrocollagenous membrane that resembles a cocoon and can

**Table 3: Transudative versus Exudative Ascites**

Type of Ascites	Common Causes	Laboratory Features	Radiologic Features
Transudative	Cirrhosis Heart failure Liver failure Budd-Chiari syndrome	Clear fluid Serum ascites albumin gradient $\geq 1.1$ g/dL No red blood cells White blood cell count $< 250/\mu\text{L}$	Fluid tracks along the adjacent viscera without loculations May be associated with pleural effusions, pericardial effusion, gallbladder wall edema, and edema of the body wall Anechoic at US Usually homogeneous with attenuation $< 20$ HU at CT High T2-weighted and low T1-weighted signal intensity at MRI
Exudative	Hemorrhage Malignancy Infection Inflammation	Variable (depends on the cause)	Usually depends on the cause Propensity for loculations and/or septa Internal echoes or septa at US Associated peritoneal thickening and/or enhancement in some cases Often heterogeneous with higher attenuation, $> 20$ – $30$ HU at CT Occasional high T1-weighted signal intensity at MRI for collections with blood products and/or proteinaceous contents

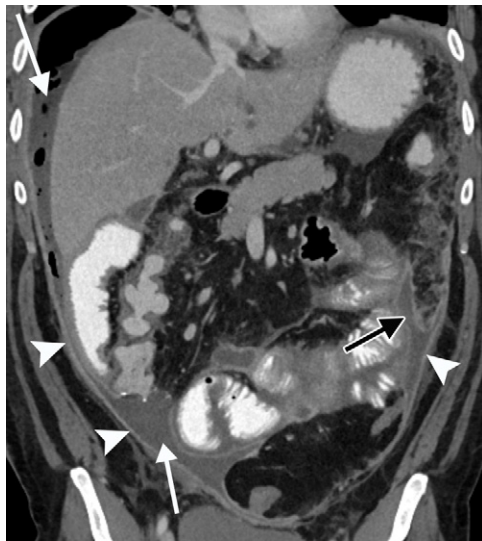


**Figure 10.** Peritonitis in a 39-year-old man who underwent ileocecectomy. Coronal contrast-enhanced CT image shows a complicated fluid collection in the peritoneal cavity, with associated diffuse peritoneal thickening (arrowheads), indicating peritonitis. Multiple trapped foci of gas and an air-fluid level are seen within the right supramesocolic space, which appear to communicate with additional fluid collections in the right paracolic gutter and right inframesocolic space (white arrows). A smaller left inframesocolic collection (black arrow) is also noted.



**Figure 11.** Rupture of multiple liver masses in a 66-year-old man who presented with acute nonlocalized abdominal pain. Sagittal contrast-enhanced CT image shows ill-defined hypoenhancing liver masses (multifocal hepatocellular carcinoma) (arrows) and associated perihepatic hemorrhage due to rupture of one of the masses. Extension of hemorrhage into the gastrohepatic ligament is noted, with substantial mass effect on the lesser curvature of the stomach (arrowheads).

lead to recurrent small bowel obstruction. This entity can occur as a complication of long-term peritoneal dialysis (Fig 19). It may also be idiopathic or associated with other conditions such as tuberculosis infection (Fig 18), abdominal surgeries, intra-abdominal shunts, or malignancies, most notably ovarian carcinoma (Fig 20). Differentiating benign from malignant causes of encapsulating peritoneal sclerosis at imaging may be difficult without a pertinent clinical history (26,53,54). Thorough clinical evaluation, imaging studies, and tissue biopsy are essential for accurately diagnosing and differentiat-

ing between neoplastic and nonneoplastic causes of peritoneal lesions to guide appropriate management (30,48).

**Pathways of Neoplastic Peritoneal Disease Spread.**—Neoplastic dissemination in the peritoneal cavity and membrane occurs through various pathways. Peritoneal seeding in peritoneal carcinomatosis is influenced by peritoneal fluid circulation dynamics, which result in tumor deposits preferentially localizing to sites of fluid stasis or reabsorption (Fig 5). Direct invasion involves tumors breaching the

**Table 4: Various Causes of Pathologic Intraperitoneal Fluid Collections**

Fluid Type	Common Causes	Salient Imaging Features and Diagnostic Pearls
Hemorrhage	Trauma Postsurgical or postprocedural Pathologic (eg, tumoral bleed) Spontaneous	CT: attenuation >30 HU (although attenuation <30 HU does not exclude hemorrhage) MRI: T1 signal hyperintensity Sentinel clot sign: hematoma preferentially accumulates at or adjacent to the source of bleeding Active contrast extravasation in cases of acute ongoing hemorrhage
Biliary ascites or biloma	Postsurgical or postprocedural Trauma	Can be confined to the right upper quadrant (biloma) or accumulate freely in the abdomen or pelvis Commonly appear as simple fluid at imaging, unless infected Confirmatory diagnosis with radionuclide imaging (HIDA) or MRI using a hepatobiliary contrast agent (eg, Eovist; Bayer) Elevated bilirubin at fluid analysis
Pancreatic ascites	Acute pancreatitis Postsurgical or postprocedural Trauma	Associated findings related to the cause of a pancreatic leak (eg, peripancreatic stranding and gallstones in cases of pancreatitis; history of recent surgery or trauma) May be associated with retroperitoneal or peripancreatic collections Elevated amylase at fluid analysis
Infectious or pyogenic	Bowel perforation Postsurgical or postprocedural Localized infection or secondary to hematogenous spread	Smooth peritoneal thickening and enhancement Loculations and localized abscess formation Mesenteric thickening US: complicated fluid with internal echoes and/or septa CT or MRI: diffuse peritoneal enhancement and rim-enhancing collections Restricted diffusion at diffusion-weighted MRI Free air and feculent collections in cases of bowel perforation
Urinoma	Trauma Postsurgical or postprocedural (eg, after kidney transplant or prostatectomy)	Most commonly due to traumatic intraperitoneal bladder rupture CT: delayed (excretory phase) imaging demonstrates contrast extravasation and accumulation CT cystography can be used for problem solving Elevated creatinine level at fluid analysis
Chylous ascites	Trauma Infiltration of lymphatics and cisterna chyli by malignancy	Generally indistinguishable from other causes of uncomplicated ascites CT: may have CT attenuation <0 HU MRI: may show high signal intensity on T1-weighted images, depending on fat content Milky appearance of ascitic fluid with elevated triglyceride levels
Malignant ascites	Peritoneal seeding by malignancy Primary peritoneal carcinomatosis	Associated with irregular and nodular peritoneal thickening Fluid loculations, mesenteric thickening, and nodularity Evidence of primary malignancy and/or other metastatic implants
Mucinous ascites	Pseudomyxoma peritonei Mucinous carcinomatosis	CT/MRI: scalloping of the visceral surface of the solid organs, most commonly the liver

serous membrane to infiltrate adjacent peritoneal layers and the peritoneal cavity. Hematogenous spread can occur when aggressive malignancies invade the vasculature and embolize to the peritoneal surface (45). Lymphatic spread involves the migration of tumor cells through lymphatic vessels, accessing the peritoneum via the lymphatic channels of the diaphragmatic surface. This route of dissemination is specifically implicated in the spread of non-Hodgkin lymphoma and ovarian and gastrointestinal cancers, for example. Also, metastatic deposits may directly involve visceral organ surfaces, such as the liver and spleen, resulting in surface nodularity, biconvex deposits, and scalloping, which can mimic primary hepatic and splenic tumors (Figs 6, 7). Metastatic spread to the ovaries can also occur through transperitoneal, hematogenous, or retrograde lymphatic routes. Regardless of the route, these metastatic implants are referred to as Krukenberg tumors, often arising from gastrointestinal tract primary malignancies (26,55,56). At imaging, these tu-

mors frequently appear as bilateral mixed solid and cystic ovarian masses (Fig S10) (57).

### Peritoneal Ligaments and Related Structures

The peritoneal ligaments, mesenteries, and omenta are commonly recognized at imaging by the major blood vessels running through them (Figs 1, 2, S2–S4) in the subperitoneal space (2,58). In addition to channeling major vessels, nerves, and lymphatic vessels, this space can also serve as a conduit for the spread of disease between organs and supporting ligaments and mesenteries (2,18).

### Disease Spread along the Peritoneal Ligaments and the Mesenteries

Various neoplastic, infectious, and inflammatory processes can spread along the peritoneal ligaments due to their proximity to the viscera from which pathologic processes often originate (Figs 16, 21–25, S11, S12) (59). Many abdominal and

**Table 5: Neoplastic Conditions of the Peritoneum**

Condition	Etiologic and Imaging Features
Peritoneal carcinomatosis	Metastatic disease to the peritoneum originating from an epithelial malignancy Manifests as peritoneal masses of varying sizes, which can be focal or diffuse Associated ascites is common and can have loculations Calcifications may be seen in serous ovarian neoplasms and after chemotherapy
Peritoneal lymphomatosis	Spread of lymphoma (commonly non-Hodgkin type) along the peritoneal lining Generally manifests as bulky homogeneous peritoneal masses Associated lymphadenopathy, with or without hepatosplenomegaly Ascites may be seen
Peritoneal sarcomatosis	Intraperitoneal seeding of sarcoma Typically manifests as bulky heterogeneous peritoneal masses Generally there is no associated lymphadenopathy Ascites may or may not be present
Primary peritoneal serous carcinoma	Epithelial neoplasm arising from the peritoneal surface, with pathologic features resembling surface ovarian neoplasms, but not arising from the ovaries Findings mimic peritoneal carcinomatosis, with peritoneal deposits, ascites, and mesenteric or omental nodules; no adnexal masses are present
Desmoplastic small round cell tumor	Typically manifests as peritoneal-based rounded masses in adolescent and young adult males No obvious organ of primary involvement to suggest metastatic spread Less commonly may manifest as an infiltrative peritoneal mass
Peritoneal malignant mesothelioma	Linked to asbestos exposure, but up to 40% can arise spontaneously Variable manifestations, with diffuse or nodular peritoneal thickening, which can be associated with omental thickening and ascites Associated pleural changes can be present in asbestos-related disease
Multicystic peritoneal mesothelioma	Controversy regarding the cause and nomenclature Different names are being used interchangeably, including <i>peritoneal inclusion cyst</i> It has been labeled by different authors as a chronic inflammatory or neoplastic process Typically affects middle-aged women; no association with asbestos exposure Manifests as unilocular or multilocular peritoneal-based homogeneous fluid-containing lesions predominantly in the pelvis No mass effect on the adjacent structures or intralésional solid components

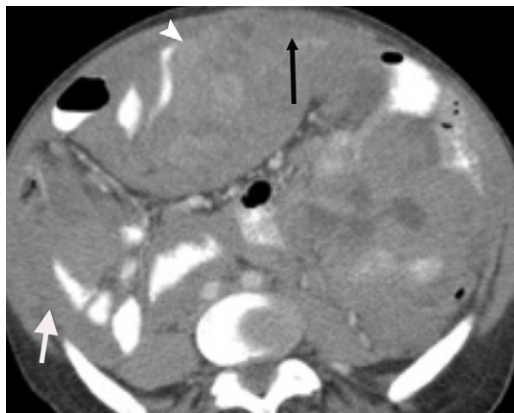


**Figure 12.** Advanced peritoneal mesothelioma in a 76-year-old woman. Axial contrast-enhanced CT image of the abdomen shows extensive nodular soft-tissue masses involving the peritoneal surfaces (white arrow) and greater omentum (black arrow). The masses are seen enveloping and displacing several small bowel loops (arrowhead) and indicate likely small bowel mesenteric and/or serosal involvement.

pelvic neoplasms, particularly gastrointestinal and ovarian malignancies, are known to spread along subperitoneal ligaments as well as along the organs they connect, allowing disease advancement into neighboring viscera (6,26). Identifying the peritoneal and mesenteric ligaments characteristically involved in a disease process and knowing their anatomic connections are crucial to systematically assessing disease spread. The primary mesenteric ligaments are discussed in the next section.

**Transverse Mesocolon.**—The transverse mesocolon is an important ligament that interconnects several peritoneal ligaments, mesenteries, and abdominal organs (Figs 26, S4). It bridges the supra- and inframesocolic ligaments (Table 1, Fig 26) and is directly contiguous with the splenorenal and phrenicocolic ligaments in the left hemiabdomen, the hepatoduodenal and the duodenocolic ligaments in the right hemiabdomen, the gastrocolic ligament superiorly, and the root of the small bowel mesentery inferiorly (Fig 26). The root of the transverse mesocolon rests horizontally along the anterior aspect of the pancreas (Figs 22, 25, 27).

The transverse mesocolon also relates closely to several abdominal organs, including the pancreas, stomach, duodenum, and colon, allowing disease spread between these organs (Figs

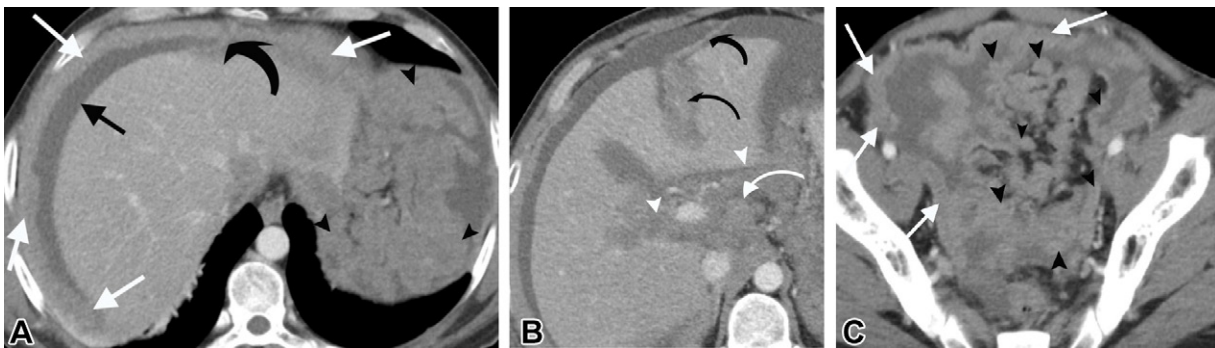


**Figure 13.** Peritoneal desmoplastic small round cell tumor in a 33-year-old man. Axial contrast-enhanced CT images of the abdomen and pelvis show diffuse, irregular, nodular peritoneal thickening (white straight arrows in **A** and **C**), which are most pronounced in the left subphrenic space (black arrowheads in **A**), with mild ascites (black straight arrow in **A**). Involvement of the peritoneal lining of the falciform ligament (curved black arrows in **A** and **B**) and hepatoduodenal ligament (white arrowheads in **B**) is noted. Multiple visceral peritoneal and mesenteric nodules (black arrowheads in **C**) are noted, with diffuse involvement of the ileal small bowel mesentery. The tumor is noted to extend into the porta hepatis region (curved white arrow in **B**).

**Figure 14.** Diffuse mesenteric metastases and peritoneal carcinomatosis from breast cancer in a 52-year-old woman. Coronal (**A**) and axial (**B**) contrast-enhanced CT images reveal diffuse tumoral involvement of the leaves of the mesentery (black arrowheads) with peritoneal masses (white arrows), diffuse peritoneal thickening (white arrowheads), serosal involvement of the small bowel loops (black arrows), and ascites.

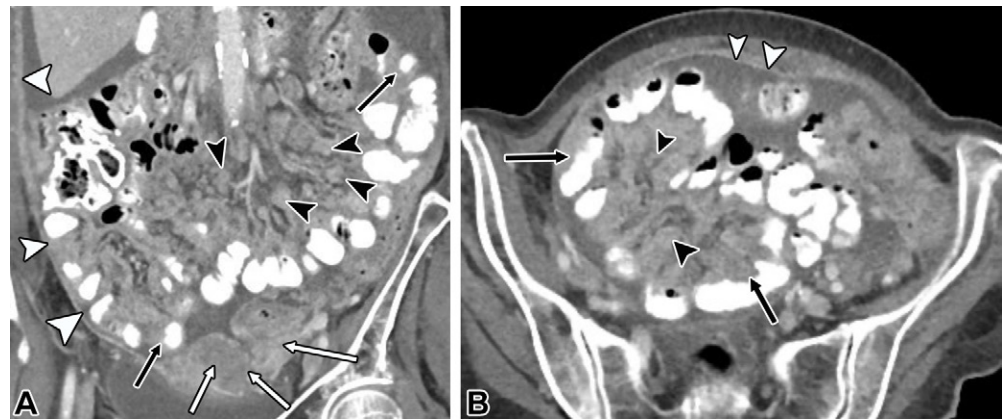
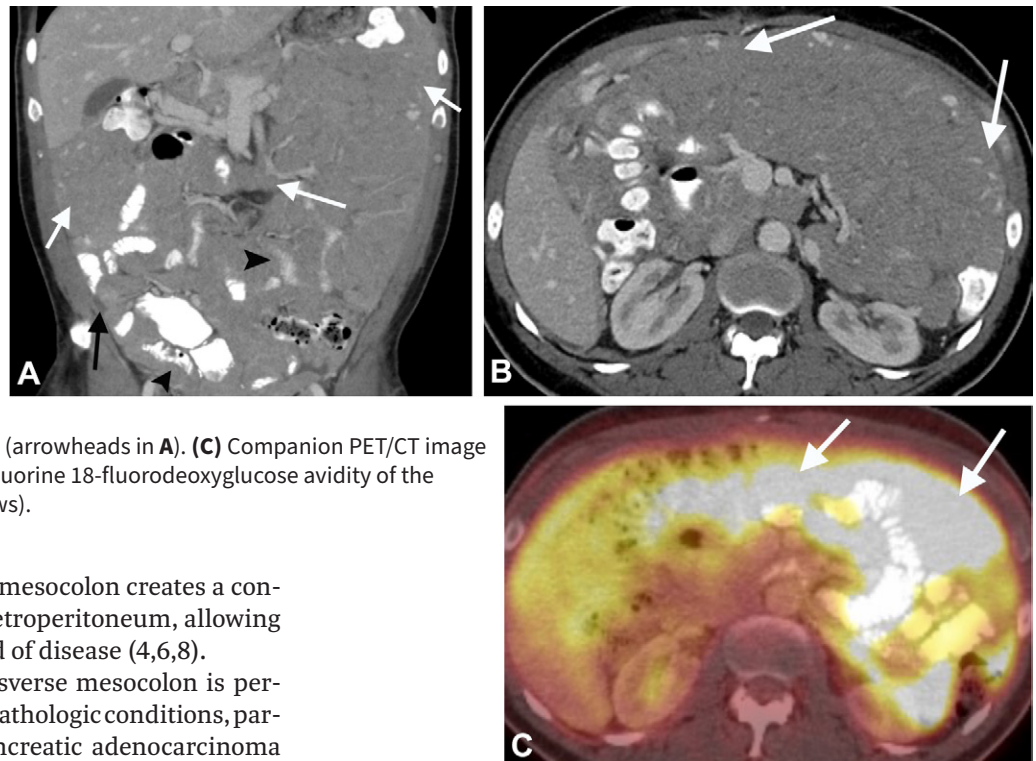


**Figure 15.** Peritoneal lymphomatosis in a 56-year-old man with a history of marginal zone lymphoma and subsequent diffuse large B-cell lymphoma transformation who presented with a low-grade fever, fatigue, abdominal pain, and swelling. (**A, B**) Coronal (**A**) and axial (**B**) contrast-enhanced CT images show extensive diffuse peritoneal low-attenuation masses (white arrows) occupying most of the abdominopelvic cavity with minimal ascites (black arrow in **A**), consistent with peritoneal lymphomatosis. There is extensive mesenteric involvement by the masses with extension to the small bowel serosa (arrowheads in **A**). (**C**) Companion PET/CT image of the mid abdomen shows substantial fluorine 18-fluorodeoxyglucose avidity of the peritoneal and mesenteric masses (arrows).



16, 22–25, 27). Lastly, the transverse mesocolon creates a connection between the stomach and retroperitoneum, allowing peritoneal-to-retroperitoneal spread of disease (4,6,8).

Disease spread through the transverse mesocolon is perhaps best exemplified in pancreatic pathologic conditions, particularly acute pancreatitis and pancreatic adenocarcinoma

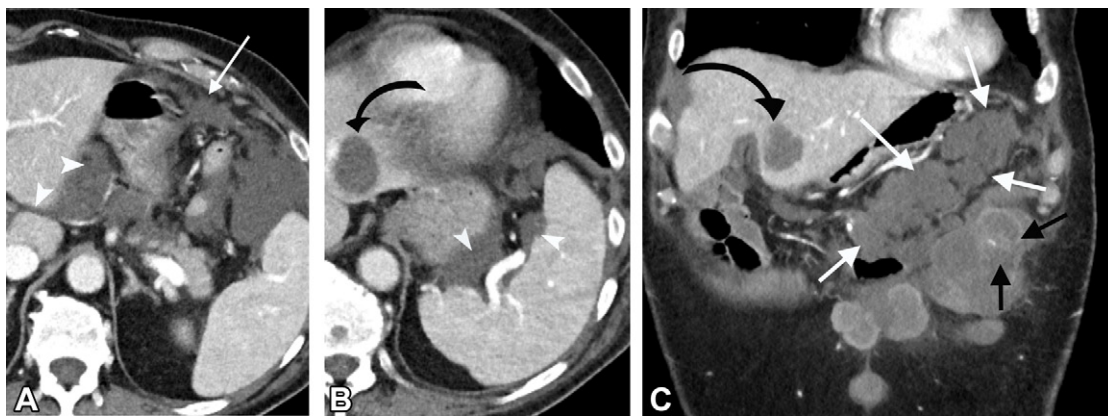


**Figure 16.** Peritoneal deposits in a 75-year-old man with a history of mucinous adenocarcinoma of the appendix. Axial (**A, B**) and coronal (**C**) contrast-enhanced CT images of the abdomen show multiple deposits involving the gastrocolic ligament (greater omentum) (white straight arrows in **A** and **C**) and the gastrohepatic ligament, with extension along the fissure of the ligamentum venosum (arrowheads in **A**). Similar deposits (white arrowheads in **B**) are seen along the gastrosplenic ligament, with invasion of the splenic hilum. There are numerous hepatic (curved black arrow in **B** and **C**) and abdominal wall (black arrow in **C**) deposits.

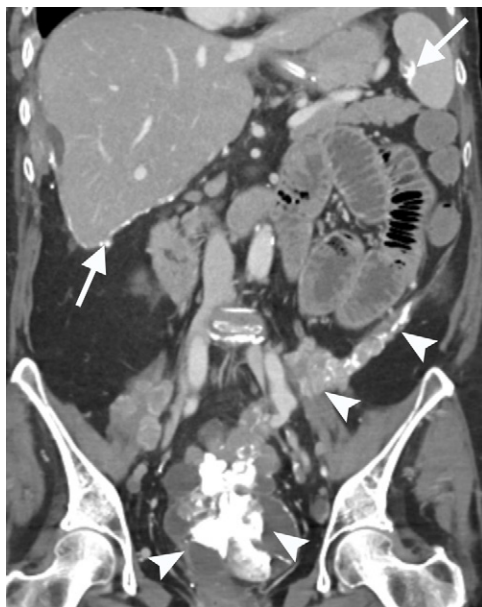


**Figure 17.** Metastases in a 68-year-old woman with a history of serous ovarian carcinoma and peritoneal carcinomatosis. Coronal contrast-enhanced CT image shows multiple abdominopelvic calcified peritoneal and mesenteric metastases (arrowheads) and multiple perihepatic and perisplenic capsular calcifications (arrows).



**Figure 18.** Tuberculous peritonitis in a 67-year-old man. Coronal contrast-enhanced CT image shows symmetric peritoneal and mesenteric thickening (white arrow), with abnormal enhancement of the peritoneal reflections (arrowhead) and high-attenuation exudative ascites (black arrow). There is a grouped "cocoon"-type morphology of small bowel loops in the central abdomen, indicating peritoneal fibrotic changes and adhesions.

(Figs 22, 25, 27). In these examples, inflammatory or malignant cells may course through the transverse mesocolon via the duodenocolic ligament into the lesser omentum (Fig S11), along the phrenicocolic ligament to the splenic flexure, via the splenorenal ligament to the splenic hilum, along the gastrocolic ligament to the lesser sac (Fig S11), and may also track inferiorly into the root of the small bowel mesentery (Figs 25, 27) (59,60). In general, ligamentous involvement tends to be more focal in patients with pancreatic adenocarcinoma (Fig 27) (59) and broader in patients with pancreatitis, especially if severe (Fig 22).

**Supramesocolic Ligaments.**—The lesser omentum includes the superior gastrohepatic and inferior hepatoduodenal ligaments, which connect the liver to the lesser curvature of the stomach and the proximal duodenum, respectively. The gastrohepatic ligament acts as a conduit for disease spread from the distal esophagus and stomach to the liver and porta hepatis. The hepatoduodenal ligament represents the free edge of the lesser omentum. It facilitates bidirectional disease spread from the hepatic hilum into the gastrohepatic

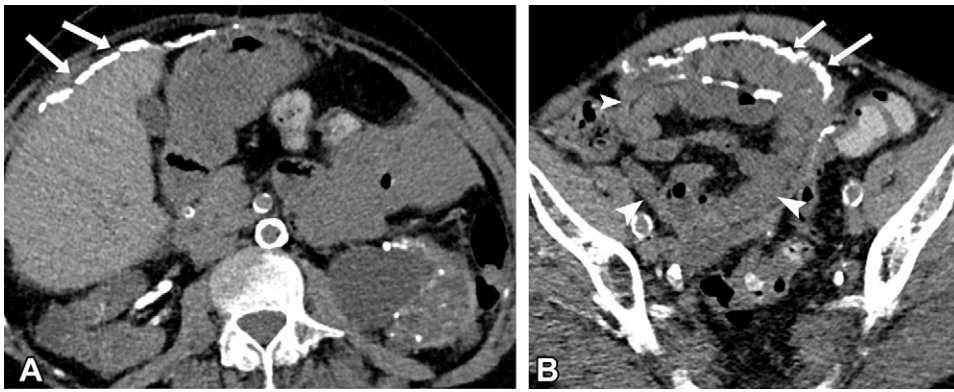


**Figure 19.** Dialysis-related encapsulating peritoneal sclerosis in a 53-year-old woman with kidney failure who was undergoing long-term dialysis. Axial CT images without intravenous contrast material show central clumping of the small bowel loops (arrowheads in **B**), with surrounding abnormal peritoneal thickening and calcifications extending along the hepatic capsule (arrows in **A** and **B**). Note the atrophic changes of both kidneys and the diffuse vascular calcifications.

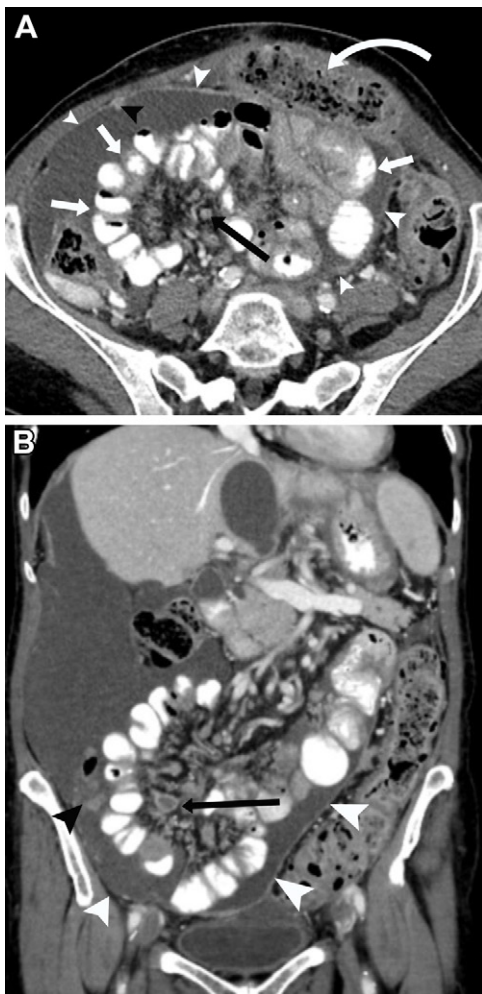


**Figure 20.** Encapsulating peritoneal sclerosis in a 77-year-old woman with ovarian cancer and peritoneal carcinomatosis. Axial (**A**) and coronal (**B**) contrast-enhanced CT images show grouping of the small bowel loops (straight white arrows in **A**) in the central portion of the abdomen. The bowel loops appear to be encased in an abnormally thickened peritoneum (white arrowheads in **A** and **B**), with anterior displacement of the transverse colon (curved white arrow in **A**). Multiple metastatic mesenteric (black arrow in **A** and **B**) and peritoneal (black arrowhead in **B**) nodules are noted together with moderate ascites.

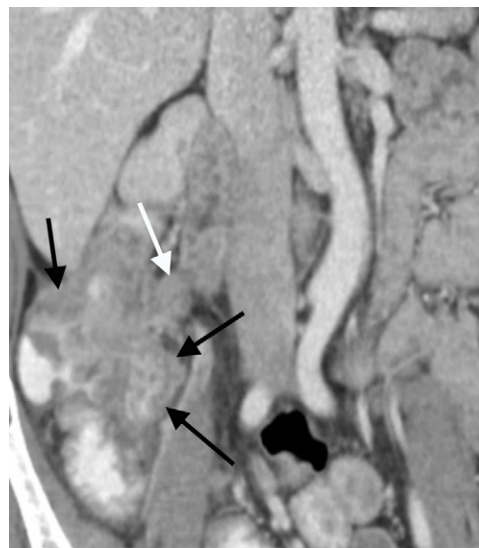


**Figure 21.** Colon cancer and subperitoneal disease spread in a 53-year-old man. Coronal contrast-enhanced CT image shows a concentric soft-tissue mass involving the hepatic flexure of the colon (black arrows). The mass encroaches on the colonic lumen and demonstrates pericolonic soft-tissue extension. Metastatic soft-tissue extension is also seen along the duodeno-colic ligament, with formation of a paraduodenal mass (white arrow).

ligament superiorly (Fig 11), through the duodenocolic ligament into the transverse mesocolon inferiorly (Fig 26), into the falciform ligament anteriorly (Fig 13), and into the greater omentum along its leftward aspect (Figs 16, 24) (6,8,61). The portal vein runs in the hepatoduodenal ligament and can be affected by neoplastic and nonneoplastic disease processes (6). In patients with advanced cancers, dissection of the hepatoduodenal ligament, with preservation of the portal vein and hepatic artery, has a high risk of leaving residual tumor and portends a poor prognosis (61).

The gastrosplenic ligament connects the greater curvature of the stomach to the splenic hilum (Figs 2, S11, S12), and the splenorenal ligament connects the splenic hilum to the left anterior pararenal space. These ligaments form a pathway for disease spread between the greater curvature of the stomach and retroperitoneal structures such as the distal pancreas (6,8).

The gastrocolic ligament (or greater omentum) attaches the greater curvature of the stomach to the transverse colon (Figs 16, 24). It relates to the hepatoduodenal ligament along its right lateral aspect and is continuous with the gastrosplenic ligament on the left. The ligament is primarily involved in pathologic conditions affecting the greater curvature of the stomach and can be secondarily involved in transverse colonic and pancreatic abnormalities (6). Omental metastatic disease, commonly referred to as “caking,” is often encountered

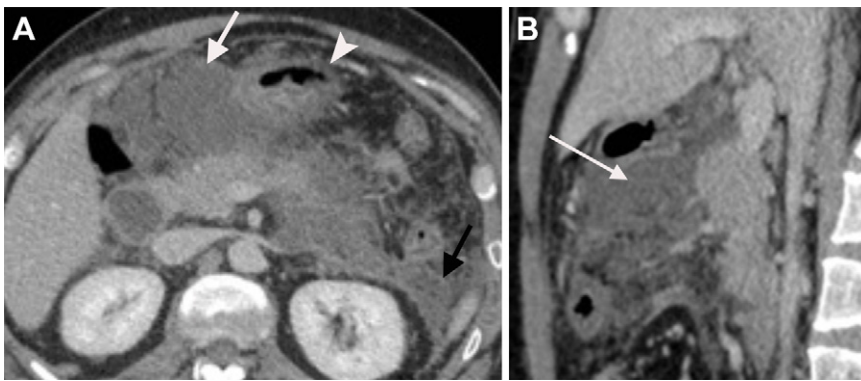


**Figure 22.** Acute pancreatitis and subperitoneal spread of inflammation in a 49-year-old man. Axial (**A**) and sagittal (**B**) contrast-enhanced CT images of the abdomen show sequelae of necrotizing pancreatitis, including extensive peripancreatic fat stranding and fluid collections (white arrow in **A**). Inflammatory changes extend through the subperitoneal space, specifically the transverse mesocolon and gastrocolic ligament (arrow in **B**). Transverse colonic wall thickening and edema (arrowhead in **A**) are also noted. Inflammation is also seen extending in the left anterior pararenal space with fluid collection and thickening of the left anterior perinephric fascia (black arrow in **A**).

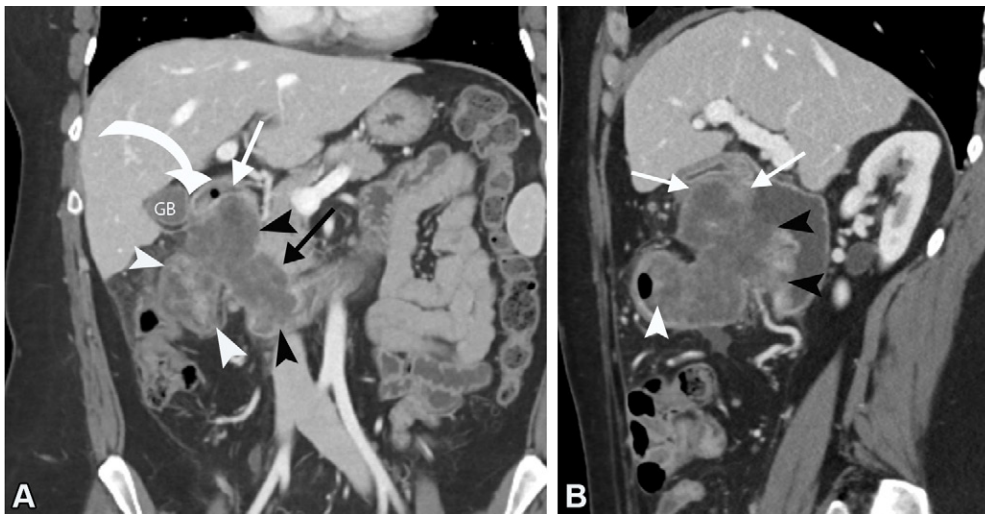


**Figure 23.** Colon cancer in a 44-year-old woman. Coronal (**A**) and sagittal (**B**) contrast-enhanced CT images show a large heterogeneous mass involving the proximal transverse colon and hepatic flexure (white arrowheads in **A** and **B**). The mass has a large exophytic component that extends along the duodenocolic ligament to involve the duodenum (black arrowheads in **A** and **B**), along the transverse mesocolon to involve the head of the pancreas (black arrow in **A**), and along the hepatoduodenal ligament to involve the gastroduodenal junction (straight white arrows in **A** and **B**) and abut the gallbladder wall (curved white arrow in **A**).

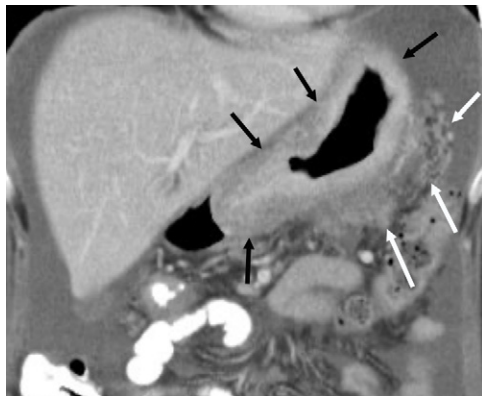


**Figure 24.** Metastatic spread in a 53-year-old man with gastric cancer. Coronal contrast-enhanced CT image shows diffuse gastric wall thickening (black arrows) with metastatic spread into the gastrocolic ligament (greater omentum) (white arrows). A moderate to large volume of ascites is noted.

in patients with peritoneal carcinomatosis due to the predominance of primitive lymphoid tissue in the greater omentum compared with other mesenteric ligaments (Fig 16) (62).

**Inframesocolic Ligaments.**—The small bowel mesentery communicates with the transverse mesocolon superiorly in

the midcentral abdomen (Fig 26). The superior portion also closely approximates the hepatoduodenal ligament. The small bowel mesentery is continuous laterally, with the ascending mesocolon on its right side and the descending mesocolon on its left side.

Diseases involving the mesentery include benign and malignant masses, infections, inflammatory conditions, and other less common abnormalities (Table 6) (Figs 25, 28–31, S13). Lymphoma is the most common solid mesenteric neoplasm. It manifests as multiple rounded soft-tissue masses, which typically surround the mesenteric vasculature or bowel without causing vascular occlusion or bowel obstruction (ie, “sandwich” sign) (Fig 29). This may also be associated with increased attenuation of the mesentery (“misty” mesentery) (63,64).

Metastatic disease generally occurs in patients with a known malignancy and often manifests as focal or conglomerate mesenteric masses of varying sizes (Figs 14, 20). Nodular soft-tissue thickening along the serosal surface of the adjacent bowel can also be seen and is often attributed to mesenteric infiltration and less often to hematogenous spread (Fig 32). In general, the degree of nodal involvement in lymphoma tends to be more extensive and diffuse than in other primary malignancies (64,65).

Neuroendocrine tumor deposits in the mesentery typically represent metastatic nodal spread from an occult primary bowel neuroendocrine tumor. Metastasis of neuroendocrine

**Table 6: Common Conditions Affecting the Mesentery**

Condition	Salient Features	Imaging Features and Pearls in Diagnosis
Lymphoma	Most common solid mesenteric neoplasm	Multiple rounded soft-tissue masses, generally demonstrating homogeneous enhancement Can manifest as bulky masses surrounding mesenteric vessels or bowel tissue, without ischemia or bowel obstruction (sandwich sign) (Fig 28) May be associated with increased attenuation of the mesentery (misty mesentery)
Metastases	Can spread to the mesentery through the multiple pathways discussed in detail in this article	Multiplicity is a typical feature Generally occur in patients with a known primary malignancy At MRI, increased intrinsic T1 signal intensity may be seen in hemorrhagic metastases or in melanoma metastases
Carcinoid tumor	Neuroendocrine tumor typically representing metastatic nodal spread (Fig 22) of an occult primary neuroendocrine tumor of bowel	Rounded mass with spiculated margins, and desmoplastic reaction that can lead to tethering of adjacent bowel (Fig 29) Arterial enhancing mass that may show calcifications (Fig 29) In some cases, a primary bowel tumor is seen as a nodular hypervascular lesion Primary tumor and metastatic lesions demonstrate uptake at dotatate PET/CT
Mesenteric desmoid	Locally invasive fibroblastic tumors Associated with familial adenomatous polyposis and Gardner syndrome	Can manifest as discrete or infiltrative masses Usually low or intermediate T2 signal intensity at MRI, but it can show high T2 signal intensity due to histologic variability Can extend across fascial planes
Sclerosing mesenteritis	Benign fibrotic or inflammatory process Disease spectrum varies from mesenteric panniculitis to retractile mesenteritis. May be immunoglobulin G4-related in some cases	Acute phase: mesenteric fat stranding, which surrounds the mesenteric vessels and nodes, with typical halo of spared fat surrounding these structures (fat halo sign); pseudocapsule surrounding the mesenteric fat stranding Chronic phase: a mass can form, with a desmoplastic reaction and/or calcifications; this can lead to venous obstruction, with formation of collaterals and tethering of bowel loops, which can cause bowel obstruction
Mesenteric trauma or injury	Can be an isolated finding or happen with other injuries Include mesenteric contusions, lacerations, and avulsions and can be associated with mesenteric vascular injuries and bowel ischemia	Imaging findings vary depending on the type of injury Mesenteric injuries manifest as high-attenuation collection in the mesentery, with or without active contrast extravasation (Fig 27) Associated bowel injury such as a bowel contusion or bowel wall defect or pneumoperitoneum may be present Bucket handle mesenteric tear: avulsion injury of the mesentery leading to secondary devascularization of the affected bowel segment

tumors in the mesentery often manifests as an arterial enhancing mass that may demonstrate calcifications, with a desmoplastic reaction that can lead to tethering of the adjacent bowel loops (Fig 30) (63,65,66).

Desmoid tumors of the mesentery are locally invasive fibroblastic tumors that have an association with familial adenomatous polyposis (Fig 31). Due to fibrotic tissue within, they usually demonstrate low or intermediate signal intensity at T2-weighted MRI. However, high T2 signal intensity may be seen in some cases due to histologic variability in the tumor contents (63–65).

Mesenteric panniculitis is a benign inflammatory process affecting the mesentery that can sometimes be associated with immunoglobulin G4-related disease. The acute phase is characterized by mesenteric fat stranding surrounding the vasculature and nodes, typically with a halo of spared fat around these structures (ie, the “fat halo” sign). A pseudocapsule surrounding the mesenteric fat stranding may be present. The chronic phase (ie, sclerosing mesenteritis) is characterized by mass formation with a desmoplastic reaction and/or calcifications that can lead to venous obstruction, with the formation of collateral vessels and tethering of bowel loops that can result in bowel obstruction (64,66).

The ascending, descending, and sigmoid mesocolons support and attach their respective parts of the colon to the posterior abdominal wall. They can be identified by means of their vascular landmarks (Table 1) (9,16).

Both the ascending and descending mesocolons are continuous with the small intestinal mesentery. The sigmoid mesocolon is continuous superiorly with the descending mesocolon and inferiorly with the mesorectum (9), allowing the spread of sigmoid colon abnormalities in both the abdomen and pelvis (6,8). Locally advanced colon cancer can invade surrounding structures, including the mesocolon (Figs 33, 34, S13). Direct invasion into the mesocolon can occur if the tumor penetrates through the serosa of the colon and extends into the adjacent mesenteric tissues (Fig 33) (67). On CT or MR images, features of direct invasion include the loss of the fat plane between the tumor and the mesocolon, soft-tissue thickening or masses in the mesocolon (Figs 33, 34), and irregularity or distortion of adjacent structures.

Colon cancer invading the mesocolon may lead to regional lymph node involvement (Fig 34). Paracolic and intermediate mesocolic lymph nodes act as primary collectors of lymphatic vessels originating from the colon, channeling lymphatic flow into principal nodes at the root of the mesentery. At imaging,

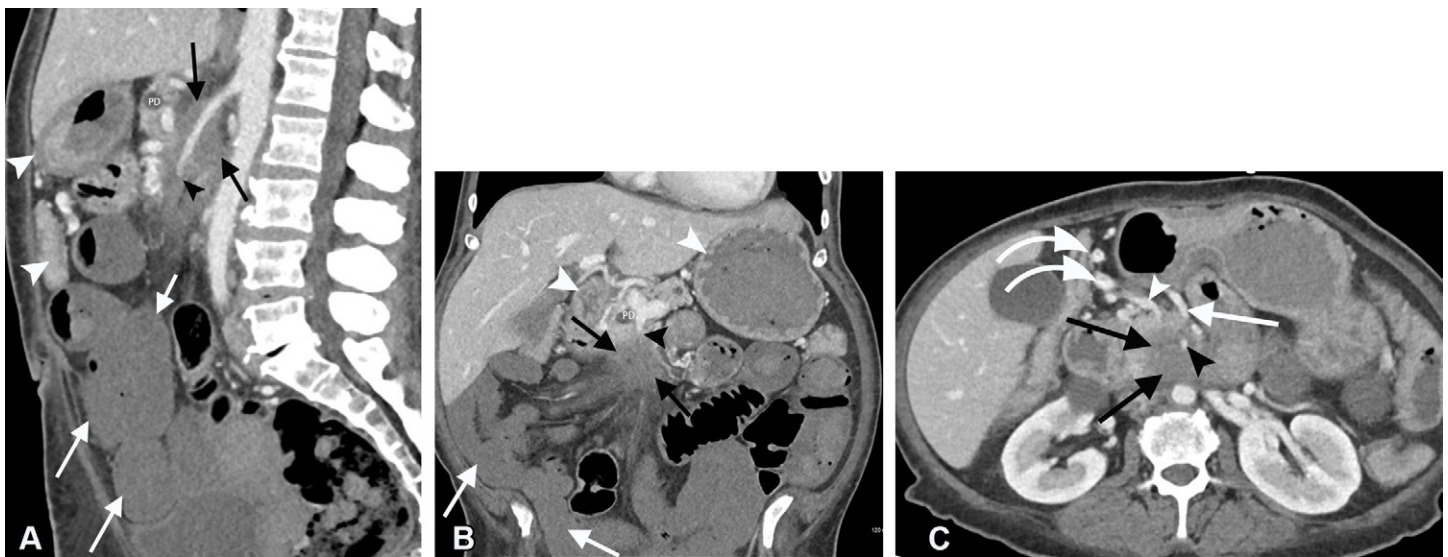


**Figure 25.** Pancreatic adenocarcinoma infiltrating the root of the small bowel mesentery and causing occlusion of the superior mesenteric artery and superior mesenteric vein, with resultant bowel ischemia in a 56-year-old woman. **(A, B)** Sagittal **(A)** and coronal **(B)** contrast-enhanced CT images show a low-attenuation pancreatic head mass. The mass infiltrates the root of the small bowel mesentery (black arrows in **A** and **B**), with abrupt occlusion of both the superior mesenteric artery (black arrowhead in **A**) and the superior mesenteric vein (black arrowhead in **B**). Dilatation of the main pancreatic duct is also seen in **B**. There are multiple nonenhancing small bowel loops (white straight arrows in **A** and **B**), denoting bowel ischemia and/or infarction (confirmed intraoperatively). Normal enhancement of the stomach and duodenum is noted (white arrowheads in **A** and **B**). **(C)** Axial contrast-enhanced CT image shows the pancreatic mass (black arrows) encasing the superior mesenteric artery (black arrowhead) and occluding the superior mesenteric vein, with associated dilatation of the middle colic vein (white straight arrow) and right gastroepiploic vein (white arrowhead). Multiple dilated collaterals veins are seen (white curved arrows).

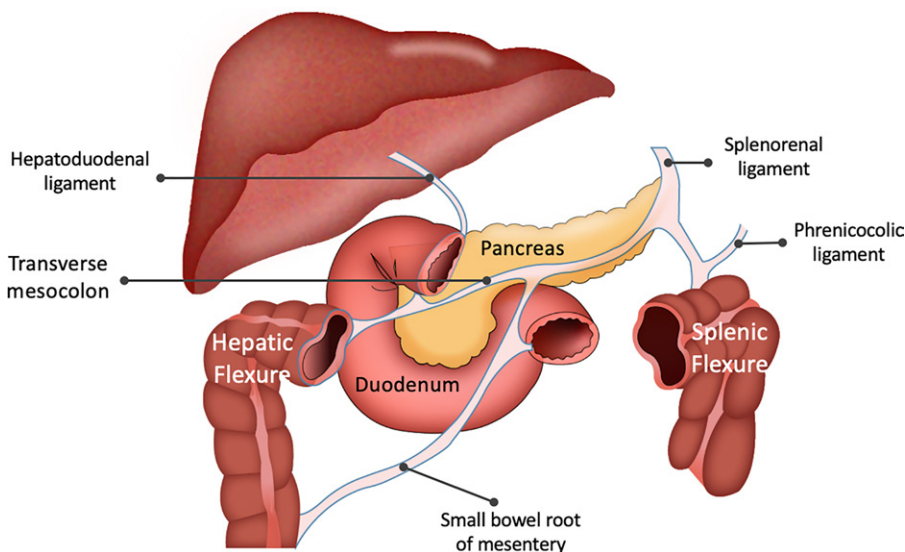


**Figure 26.** Illustration shows the transverse mesocolon and its related structures. The transverse mesocolon is an important anatomic landmark that has interconnections to several peritoneal ligaments, mesenteries, and abdominal organs.

these lymph nodes are discernible alongside the branches of the superior and inferior mesenteric vessels in the mesocolons (Fig 34) (68).

Direct invasion of the mesocolon by colon cancer may affect the treatment strategy. In these patients, complete excision of the mesocolon is the preferred treatment option. It involves removal of the diseased colon segment, the entire mesocolon, and its associated lymph nodes and blood vessels. This technique is aimed to improve outcomes and reduce the risk of local recurrence compared with traditional colon resection techniques (67,68).

### Perineural Spread

Perineural spread refers to a process by which malignant cells infiltrate nerves and then use them as a conduit for spread to nearby tissues or potentially distant sites. This pathway of disease spread is not as well understood as other routes (69).

Microscopic perineural invasion is often encountered histopathologically before manifesting at imaging, making accurate diagnosis quite challenging. However, macroscopic disease may appear as nodular thickening of involved nerves or, if the nerves themselves are not visible, as abnormal soft-tissue thickening extending along blood vessels adjacent to the primary tumor. In pancreatic malignancy, for instance, this



**Figure 27.** Subperitoneal disease spread in a 63-year-old man with a history of pancreatic adenocarcinoma. Axial contrast-enhanced CT image shows a large heterogeneously enhancing pancreatic head mass (arrow) spreading along the root of the small bowel mesentery and the transverse mesocolon, as evidenced by encasement of the superior mesenteric vein (black arrowhead) and middle colic vein (white arrowhead).

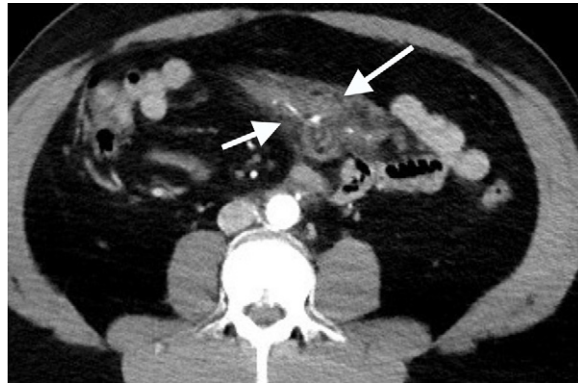


**Figure 28.** Blunt abdominal trauma in a 39-year-old man who presented after being an unrestrained backseat passenger in a high-speed motor vehicle crash. Axial contrast-enhanced CT image shows a large triangular-shaped area of high attenuation involving the root of the mesentery, the surrounding branches of the superior mesenteric artery, and the superior mesenteric vein as well as the origin of the inferior mesenteric artery (arrows). Distal mesenteric vessels are poorly defined. Findings are consistent with traumatic injury of the root of the small bowel mesentery and the transverse mesocolon.



**Figure 29.** Mesenteric lymphoma in a 68-year-old woman. Sagittal contrast-enhanced pretreatment CT image (A) of the abdomen shows a large conglomerate mass (arrows) involving the root of the small bowel mesentery and extending along the course of the encased superior mesenteric vessels. The mass was biopsied and confirmed to be lymphoma. Sagittal posttreatment contrast-enhanced CT image (B) shows a substantial decrease in the size of the mesenteric mass, with residual soft tissue encircling the superior mesenteric vessels (arrowheads).

type of soft-tissue thickening may be encountered along the course of the superior mesenteric artery (Figs 25, S14) (22). Additional examples of perineural disease spread in the abdomen have been reported in cases of biliary, colorectal, gastric, prostatic, and cervical cancers as well as in lymphoma and some abdominal sarcomas (59,61–63). Clinically, perineural disease spread may manifest with neuropathic pain (70).

Perineural invasion has substantial implications for both prognosis and treatment planning. It is generally considered a poor prognostic factor with a high risk of recurrence rate (71). A multidisciplinary approach involving oncologists, surgeons, radiologists, and pathologists is often necessary for proper diagnosis and management of these cases (22).

### Lymphatic and Lymphovascular Spread

Lymphovascular spread refers to disease spread along lymphatic channels and small blood vessels in the subperitoneal space (Figs 33, S13, S14). Many malignancies can propagate in this manner, with malignant cells coursing along lymphatic channels and blood vessels in the subperitoneum of multiple mesenteries and ligaments (Figs 25, 29, 33, 34, S13, S14) (6,8).

In cases of pancreatic adenocarcinoma, as a pertinent example, patterns of subperitoneal lymphovascular spread are determined by the site of the primary tumor. In cases involving the head or uncinate process, tumor spread usually occurs along the superior mesenteric artery and the root of the mesentery (Figs 25, 27), while body and tail tumors often

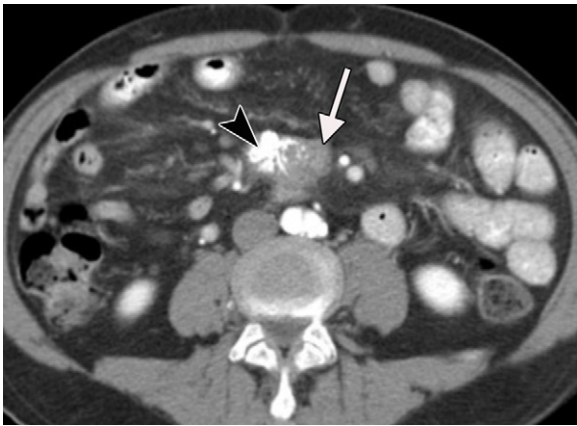


**Figure 30.** Mesenteric metastases in a 70-year-old man with a history of a small bowel carcinoid tumor. Axial contrast-enhanced CT image shows a spiculated mesenteric soft-tissue mass (arrow), with associated coarse calcifications (arrowhead). The primary presumed small bowel tumor was not identified radiographically.

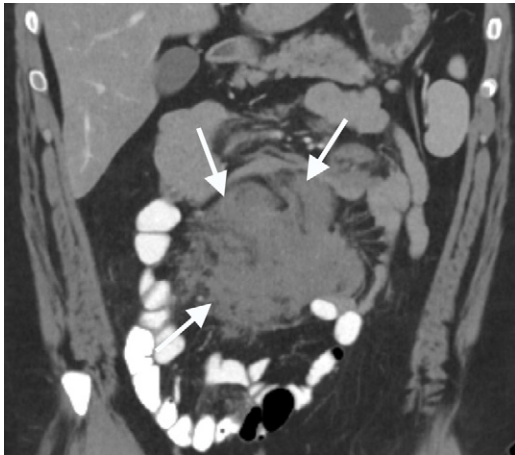


**Figure 31.** Desmoid tumor in a 33-year-old man with a history of familial colonic polyposis and both Lynch and Gardner syndromes. Coronal contrast-enhanced CT image shows a large solid and infiltrative mesenteric mass in the mid abdomen. The mass is seen encasing the mesenteric vessels and displacing surrounding bowel loops (arrows). The mass has an anterior abdominal wall component (not shown) that was biopsied and proved to represent a desmoid tumor.

involve the celiac, hepatic, and splenic arteries. Encasement of the portal vein and its confluence can also be seen.

Tumor cells from primary bowel malignancies may limit or obstruct flow in adjacent lymphatic vessels. On CT images, this can manifest as bowel wall thickening and edema, thickened mucosal folds, loss of colonic haustrations, and increased attenuation, or stranding, of surrounding mesenteric fat (Figs 33, 34) (6). In advanced cases, nodular tumor deposits in the bowel wall, with resulting luminal narrowing (Fig 21) and regional metastatic lymphadenopathy (Fig 34), can be observed (72,73). Similar to perineural disease involvement, the presence of lymphovascular spread at imaging portends a

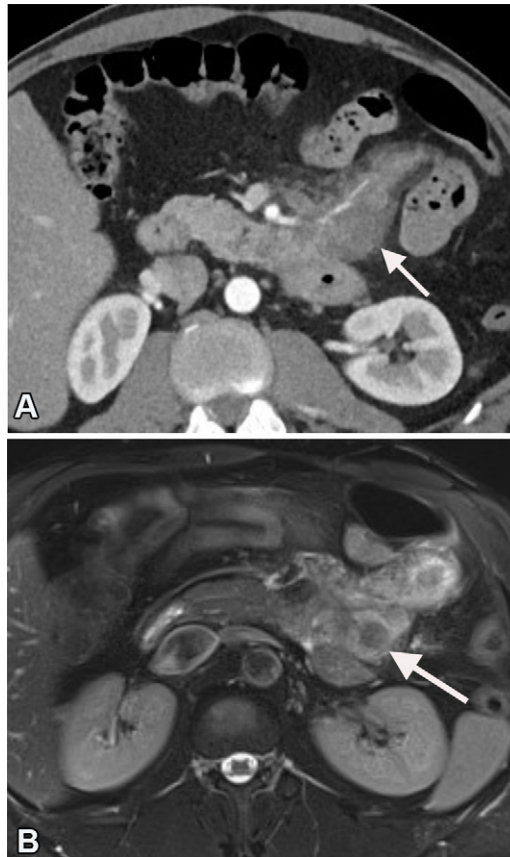


**Figure 32.** Metastatic melanoma to the small bowel mesentery in a 79-year-old man. **(A)** Axial contrast-enhanced CT image shows proximal small bowel wall nodular thickening (arrow). The initial differential diagnosis included a small bowel wall hematoma versus a neoplasm. **(B)** Axial T2-weighted MR image shows small bowel wall thickening and surrounding lymphadenopathy. Lymph nodes show low signal intensity (arrow). The mass was biopsied and proved to be metastatic melanoma.

poor prognosis and may substantially alter management decisions (74).

## Conclusion

The anatomy of the peritoneum, subperitoneum, and related ligaments and spaces is complex. The peritoneal cavity and its fluid flow dynamics, membranes, peritoneal ligaments, and subperitoneal spaces form potential spaces and pathways for the spread of a myriad of neoplastic and nonneoplastic abnormalities. Understanding the embryology, anatomy, and various classifications of the peritoneum is crucial for recognizing and accurately describing patterns of disease spread in the peritoneum. This structured analysis provides radiologists with a framework for navigating the complex anatomy and patterns of pathologic dissemination in the abdomen and pelvis.

**Author affiliations.**—From the Department of Diagnostic Imaging, The University of Texas MD Anderson Cancer Center, 1515 Holcombe Blvd, Houston, TX 77030 (A.H.G., M.B., K.M.E.); Department of Radiology, University of Menoufia, Menoufia, Egypt (M.A.); Department of Radiology, University of Missouri, Columbia, Mo (I.A.K., E.A.S.M.); Department of Radiology, Vanderbilt University Medical Center, Nashville, Tenn (N.P.G.); Department of Radiology, Cork University Hospital, Cork, Ireland (J.S.); Department of Radiology, Cleveland Clinic, Cleveland, Ohio (P.S.L.); and Department of Diagnostic Imaging, Mayo Clinic, Jacksonville, Fla (M.H.). Presented as an education exhibit at the 2022 RSNA Annual Meeting. Received September 18, 2023; revision requested February 16, 2024, and received April 3; accepted April 16. **Address correspondence to** A.H.G. (email: [ahgaballah@mdanderson.org](mailto:ahgaballah@mdanderson.org)).

**Disclosures of conflicts of interest.**—K.M.E. Editorial board member of *Radiographics*. All other authors, the editor, and the reviewers have disclosed no relevant relationships.

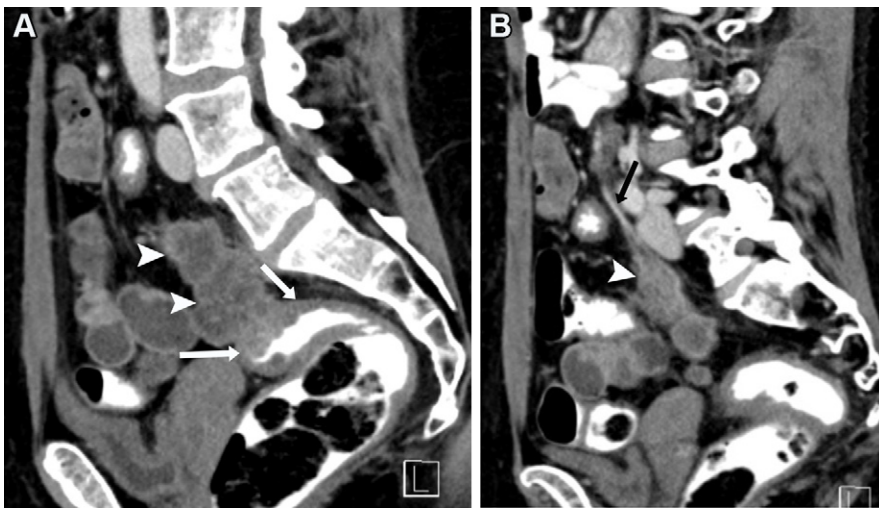


**Figure 33.** Sigmoid colon cancer in a 56-year-old woman. Sagittal contrast-enhanced CT images show asymmetric wall thickening of the sigmoid colon (arrows in **A**), with an exophytic mass invading the sigmoid mesocolon (arrowheads in **A** and **B**). Soft-tissue nodularity is seen extending along the branches of the inferior mesenteric vessels (arrow in **B**), which is suggestive of perivascular spread.

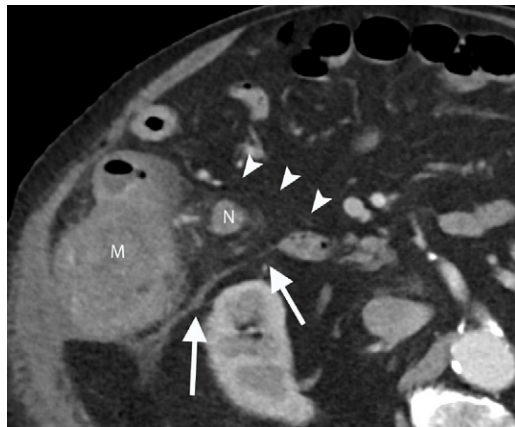


**Figure 34.** Nodal metastasis in the ascending mesocolon in an 83-year-old man with colon cancer. Axial contrast-enhanced CT image shows an ascending colonic mass (*M*) and an enlarged lymph node (*N*) in the ascending mesocolon. The lymph node is bordered anteriorly by the parietal peritoneum (arrowheads) and posteriorly by the anterior pararenal fascia (arrows). Inflammatory changes in the form of fat stranding in the right lower quadrant are secondary to perforation of the colonic mass into the retroperitoneum with formation of a retroperitoneal abscess (not shown). Thickening of the right anterior perinephric fascia could be secondary to reactive inflammation and/or infiltration by the colonic mass.

## References

1. Sugarbaker PH. Peritoneum and Peritoneal cavity. In: Standring S, ed. Gray's Anatomy. 41 British. Philadelphia, Pa: Elsevier, 2016; 1559–1673s.
2. Meyers M, Charnsangavej C, Oliphant M. Mechanism of Spread of Disease in the Abdomen and Pelvis. In: Meyers M, Charnsangavej C, Oliphant M, eds. Meyer's Dynamic Radiology of the Abdomen. 6th ed. New York: Springer-Verlag, 2011; 41–68.
3. Ba-Ssalamah A, Fakhrai N, Baroud S, Shirkhoda A. Mesentery, Omentum, Peritoneum: Embryology, Normal Anatomy and Anatomic Variants. In: Abdominal Imaging. Berlin, Heidelberg: Springer Berlin Heidelberg, 2013; 1563–1576.
4. Brink JA, Wagner BJ. Pathways for the Spread of Disease in the Abdomen and Pelvis. Springer Cham, 2023; 229–239.
5. Standring S. Peritoneum, mesentery and peritoneal cavity. In: Standring S, ed. Gray's Anatomy: The Anatomical Basis of Clinical Practice. 42nd ed. Kidlington, Oxford: Elsevier, 2021; 1150–1159.e3.
6. Ecanow J, Ivanovic AM, Gore RM, Meyers MA, Rabin DN. Pathways of Abdominal and Pelvic Disease Spread. In: Gore R, ed. Textbook of Gastrointestinal Radiology. Fifth. Philadelphia, PA: Elsevier, 2021; 999–1016.
7. Le O. Patterns of peritoneal spread of tumor in the abdomen and pelvis. World J Radiol 2013;5(3):106–112.
8. Le O. Peritoneal Cavity and Gastrointestinal Tract. In: Silverman PM, ed. Oncologic Imaging: A Multidisciplinary Approach. Second. Philadelphia, PA: Elsevier, 2023; 575–586.
9. Dalla Pria HRF, Torres US, Velloni F, et al. The Mesenteric Organ: New Anatomical Concepts and an Imaging-based Review on Its Diseases. Semin Ultrasound CT MR 2019;40(6):515–532.
10. Tirkes T, Sandrasegaran K, Patel AA, et al. Peritoneal and retroperitoneal anatomy and its relevance for cross-sectional imaging. Radiographics 2012;32(2):437–451.
11. Solass W, Struller F, Horvath P, Königsrainer A, Sipos B, Weinreich FJ. Morphology of the peritoneal cavity and pathophysiological consequences. Pleura Peritoneum 2016;1(4):193–201.
12. Patel RR, Planche K. Applied peritoneal anatomy. Clin Radiol 2013;68(5):509–520.
13. Elsayes KM, Staveteig PT, Narra VR, Leyendecker JR, Lewis JS Jr, Brown JJ. MRI of the peritoneum: spectrum of abnormalities. AJR Am J Roentgenol 2006;186(5):1368–1379.
14. Kastelein AW, Vos LMC, de Jong KH, et al. Embryology, anatomy, physiology and pathophysiology of the peritoneum and the peritoneal vasculature. Semin Cell Dev Biol 2019;92:27–36.
15. Blackburn SC, Stanton MP. Anatomy and physiology of the peritoneum. Semin Pediatr Surg 2014;23(6):326–330.
16. Coffey JC, Byrnes KG, Dockery P, Walsh D. The mesentery and the mesenteric model of abdominal compartmentalization. In: Standring S, ed. Gray's Anatomy: The Anatomical Basis of Clinical Practice. 42nd ed. Kidlington, Oxford: Elsevier, 2021; 1330.e3–1330.e7.
17. Byrnes KG, Cullivan O, Walsh D, Coffey JC. The Development of the Mesenteric Model of Abdominal Anatomy. Clin Colon Rectal Surg 2022;35(4):269–276.
18. Pannu HK, Oliphant M. The subperitoneal space and peritoneal cavity: basic concepts. Abdom Imaging 2015;40(7):2710–2722.
19. Byrnes KG, Walsh D, Walsh LG, et al. The development and structure of the mesentery. Commun Biol 2021;4(1):982.
20. Rudralingam V, Footitt C, Layton B. Ascites matters. Ultrasound 2017;25(2):69–79.
21. Lin H, Piccoli D. Ascites. In: Pediatric Gastrointestinal and Liver Disease. Elsevier, 2021; 168–178.e5.
22. Ecanow JS, Gore RM, Silvers RI, Newmark GM, Gore MD. Ascites and Peritoneal Fluid Collections. In: Gore RM, ed. Textbook of Gastrointestinal Radiology. Fifth. Philadelphia, PA: Elsevier, 2021; 1017–1025.
23. Meyers MA, Mindelzun RE. Peritoneal Reflections, Ligaments, Recesses, and Mesenteries. In: Medical Radiology. Springer, Berlin, Heidelberg; 2000: 159–182.
24. Patel CM, Sahdev A, Reznick RHCT. CT, MRI and PET imaging in peritoneal malignancy. Cancer Imaging 2011;11(1):123–139.
25. Fonseca C, Carvalho S, Cunha TM, Gil RT, Abecasis N. The many faces of pseudomyxoma peritonei: a radiological review based on 30 cases. Radiol Bras 2019;52(6):372–377.

26. Diop AD, Fontarensky M, Montoriol PF, Da Ines D. CT imaging of peritoneal carcinomatosis and its mimics. *Diagn Interv Imaging* 2014;95(9):861–872.
27. Hainaux B, Agneessens E, Bertinotti R, et al. Accuracy of MDCT in predicting site of gastrointestinal tract perforation. *AJR Am J Roentgenol* 2006;187(5):1179–1183.
28. Ilyas M, Bashir M, Robbani I, Rasool SR, Shera FA, Hamid I. Sentinel clot sign in hemoperitoneum. *Abdom Radiol (NY)* 2019;44(5):1955–1956.
29. Le O, Elsayes KM. The Peritoneum. In: *Cross-Sectional Imaging of the Abdomen and Pelvis*. New York, NY: Springer New York, 2015; 453–482.
30. Pickhardt PJ, Perez AA, Elmohr MM, Elsayes KM. CT imaging review of uncommon peritoneal-based neoplasms: beyond carcinomatosis. *Br J Radiol* 2021;94(1119):20201288.
31. Chapman BC, McIntosh KE, Jones EL, Wells D, Stiegmann GV, Robinson TN. Postoperative pneumoperitoneum: is it normal or pathologic? *J Surg Res* 2015;197(1):107–111.
32. Gayer G, Jonas T, Apter S, Amitai M, Shabtai M, Hertz M. Postoperative pneumoperitoneum as detected by CT: prevalence, duration, and relevant factors affecting its possible significance. *Abdom Imaging* 2000;25(3):301–305.
33. Leturia Etxeberria M, Biurrun Mancisidor MC, Ugarte Nuño A, et al. Imaging assessment of ectopic gas collections. *RadioGraphics* 2020;40(5):1318–1338.
34. Singh JP, Steward MJ, Booth TC, Mukhtar H, Murray D. Evolution of imaging for abdominal perforation. *Ann R Coll Surg Engl* 2010;92(3):182–188.
35. Lee CH, Kim JH, Lee MR. Postoperative pneumoperitoneum: guilty or not guilty? *J Korean Surg Soc* 2012;82(4):227–231.
36. Yagan N, Auh YH, Fisher A. Extension of air into the right perirenal space after duodenal perforation: CT findings. *Radiology* 2009;250(3):740–748.
37. Rudler M, Mallet M, Sultanik P, Bouzbib C, Thabut D. Optimal management of ascites. *Liver Int* 2020;40(Suppl 1):128–135.
38. Jafri SM, Gordon SC. Care of the cirrhotic patient. *Infect Dis Clin North Am* 2012;26(4):979–994.
39. Gore RM, Silvers RI, Newmark GM, Gore MD. Ascites and Peritoneal Fluid Collections. In: *Textbook of Gastrointestinal Radiology, 2-Volume Set*. Elsevier, 2015; 2024–2035.
40. Lipsky MS, Sternbach MR. Evaluation and initial management of patients with ascites. *Am Fam Physician* 1996;54(4):1327–1333.
41. Thoeni RF. The role of imaging in patients with ascites. *AJR Am J Roentgenol* 1995;165(1):16–18.
42. Gaballah AH, Kazi IA, Zaheer A, et al. Imaging after Pancreatic Surgery: Expected Findings and Postoperative Complications. *RadioGraphics* 2024;44(1):e230061.
43. Simbrunner B, Mandorfer M, Trauner M, Reiberger T. Gut-liver axis signaling in portal hypertension. *World J Gastroenterol* 2019;25(39):5897–5917.
44. Copelan A, Bahoura L, Tardy F, Kirsch M, Sokhandon F, Kapoor B. Etiology, Diagnosis, and Management of Bilomas: A Current Update. *Tech Vasc Interv Radiol* 2015;18(4):236–243.
45. Miguez González J, Calaf Forn F, Pelegrí Martínez L, et al. Primary and secondary tumors of the peritoneum: key imaging features and differential diagnosis with surgical and pathological correlation. *Insights Imaging* 2023;14(1):115.
46. Levy AD, Arnáiz J, Shaw JC, Sobin LH. From the archives of the AFIP: primary peritoneal tumors: imaging features with pathologic correlation. *RadioGraphics* 2008;28(2):583–607; quiz 621–622.
47. Cabral FC, Krajewski KM, Kim KW, Ramaiya NH, Jagannathan JP. Peritoneal lymphomatosis: CT and PET/CT findings and how to differentiate between carcinomatosis and sarcomatosis. *Cancer Imaging* 2013;13(2):162–170.
48. Miguez González J, Calaf Forn F, Pelegrí Martínez L, et al. Primary and secondary tumors of the peritoneum: key imaging features and differential diagnosis with surgical and pathological correlation. *Insights Imaging* 2023;14(1):115.
49. Zulfiqar M, Shetty A, Tsai R, Gagnon MH, Balfé DM, Mellnick VM. Diagnostic Approach to Benign and Malignant Calcifications in the Abdomen and Pelvis. *RadioGraphics* 2020;40(3):731–753.
50. Naeem M, Menias CO, Cail AJ, et al. Imaging Spectrum of Granulomatous Diseases of the Abdomen and Pelvis. *RadioGraphics* 2021;41(3):783–801.
51. Smoot T, Revels J, Soliman M, et al. Abdominal and pelvic splenosis: atypical findings, pitfalls, and mimics. *Abdom Radiol (NY)* 2022;47(3):923–947.
52. Muehler MR, Rendell VR, Bergmann LL, Winslow ER, Reeder SB. Ferumoxyl-enhanced MR imaging for differentiating intrapancreatic splenules from other tumors. *Abdom Radiol (NY)* 2021;46(5):2003–2013.
53. Isacson R, Segal A, Alberton J, Reinus C, Schwarz A, Grenader T. Abdominal cocoon: a potential pitfall in patients with ovarian carcinoma. *Tumori* 2012;98(6):176e–178e.
54. Singhal M, Krishna S, Lal A, et al. Encapsulating Peritoneal Sclerosis: The Abdominal Cocoon. *RadioGraphics* 2019;39(1):62–77.
55. Shah B, Tang W, Karn S. An Up-to-Date Understanding of the “Krukenberg Tumor” Mechanism. *Advances in Reproductive Sciences* 2016;04(02):31–36.
56. Agnes A, Biondi A, Ricci R, Gallotta V, D’Ugo D, Persiani R. Krukenberg tumors: Seed, route and soil. *Surg Oncol* 2017;26(4):438–445.
57. Karaosmanoglu AD, Onur MR, Salman MC, et al. Imaging in secondary tumors of the ovary. *Abdom Radiol (NY)* 2019;44(4):1493–1505.
58. Meyers MA, Oliphant M, Berne AS, Feldberg MA. The peritoneal ligaments and mesenteries: pathways of intraabdominal spread of disease. *Radiology* 1987;163(3):593–604.
59. Vikram R, Balachandran A, Bhosale PR, Tamm EP, Marcal LP, Charnsangavej C. Pancreas: peritoneal reflections, ligamentous connections, and pathways of disease spread. *RadioGraphics* 2009;29(2):e34.
60. Van Minnen LP, Besselink MGH, Bosscha K, Van Leeuwen MS, Schipper MEI, Gooszen HG. Colonic involvement in acute pancreatitis. A retrospective study of 16 patients. *Dig Surg* 2004;21(1):33–38; discussion 39–40.
61. Ota T, Araida T, Yamamoto M, Takasaki K. Operative outcome and problems of right hepatic lobectomy with pancreatoduodenectomy for advanced carcinoma of the biliary tract. *J Hepatobiliary Pancreat Surg* 2007;14(2):155–158.
62. Liu J, Geng X, Li Y. Milky spots: omental functional units and hotbeds for peritoneal cancer metastasis. *Tumour Biol* 2016;37(5):5715–5726.
63. Gopalan S, Raghu V. Unravelling the Mysteries of the Mesentery. *Journal of Gastrointestinal and Abdominal Radiology* 2021;04(01):033–048.
64. Sheth S, Horton KM, Garland MR, Fishman EK. Mesenteric Neoplasms: CT Appearances of Primary and Secondary Tumors and Differential Diagnosis. *RadioGraphics* 2003;23(2):457–473.
65. Dufay C, Abdelli A, Le Pennec V, Chiche L. Mesenteric tumors: Diagnosis and treatment. *J Visc Surg* 2012;149(4):e239–e251.
66. Kernizan AL, Revels J, Hajdu C, Manning M, Taffel MT. Mesenteric Pathologic Conditions: Interactive Case-based Approach. *RadioGraphics* 2023;43(12):e230077.
67. Fingerhut A, Tzu-Liang Chen W, Boni L, Uranues S. Complete mesocolic excision for colonic cancer. *Minerva Chir* 2019;74(2):148–159.
68. Konishi T, You YN. Complete Mesocolic Excision and Extent of Lymphadenectomy for the Treatment of Colon Cancer. *Surg Oncol Clin N Am* 2022;31(2):293–306.
69. Tu W, Gottumukkala RV, Schieda N, Lavallée L, Adam BA, Silverman SG. Perineural Invasion and Spread in Common Abdominopelvic Diseases: Imaging Diagnosis and Clinical Significance. *RadioGraphics* 2023;43(7):e220148.
70. Finnerup NB, Kuner R, Jensen TS. Neuropathic pain: From mechanisms to treatment. *Physiol Rev* 2021;101(1):259–301.
71. Chen SH, Zhang BY, Zhou B, Zhu CZ, Sun LQ, Feng YJ. Perineural invasion of cancer: a complex crosstalk between cells and molecules in the perineural niche. *Am J Cancer Res* 2019;9(1):1–21.
72. Tan CH, Vikram R, Boonsirikamchai P, et al. Extramural venous invasion by gastrointestinal malignancies: CT appearances. *Abdom Imaging* 2011;36(5):491–502.
73. Cho HS, Ahn JH. Nomenclature and Lymphatic Drainage Patterns of Abdominal Lymph Nodes. *J Korean Soc Radiol* 2022;83(6):1240–1258.
74. Al-Sukhni E, Attwood K, Gabriel EM, LeVea CM, Kanehira K, Nurkin SJ. Lymphovascular and perineural invasion are associated with poor prognostic features and outcomes in colorectal cancer: A retrospective cohort study. *Int J Surg* 2017;37:42–49.